REPORT

De Novo and Inherited Mutations in *COL4A2*, Encoding the Type IV Collagen α2 Chain Cause Porencephaly

Yuriko Yoneda,[1] Kazuhiro Haginoya,[2,3] Hiroshi Arai,[4] Shigeo Yamaoka,[5] Yoshinori Tsurusaki,[1] Hiroshi Doi,[1] Noriko Miyake,[1] Kenji Yokochi,[6] Hitoshi Osaka,[7] Mitsuhiro Kato,[8] Naomichi Matsumoto,[1] and Hirotomo Saitsu[1,*]

Porencephaly is a neurological disorder characterized by fluid-filled cysts or cavities in the brain that often cause hemiplegia. It has been suggested that porencephalic cavities result from focal cerebral degeneration involving hemorrhages. De novo or inherited heterozygous mutations in *COL4A1*, which encodes the type IV α1 collagen chain that is essential for structural integrity for vascular basement membranes, have been reported in individuals with porencephaly. Most mutations occurred at conserved Gly residues in the Gly-Xaa-Yaa repeats of the triple-helical domain, leading to alterations of the α1α1α2 heterotrimers. Here we report on two individuals with porencephaly caused by a heterozygous missense mutation in *COL4A2*, which encodes the type IV α2 collagen chain. Mutations c.3455G>A and c.3110G>A, one in each of the individuals, cause Gly residues in the Gly-Xaa-Yaa repeat to be substituted as p.Gly1152Asp and p.Gly1037Glu, respectively, probably resulting in alterations of the α1α1α2 heterotrimers. The c.3455G>A mutation was found in the proband's mother, who showed very mild monoparesis of the left upper extremity, and the maternal elder uncle, who had congenital hemiplegia. The maternal grandfather harboring the mutation is asymptomatic. The c.3110G>A mutation occurred de novo. Our study confirmed that abnormalities of the α1α1α2 heterotrimers of type IV collagen cause porencephaly and stresses the importance of screening for *COL4A2* as well as for *COL4A1*.

Porencephaly (MIM 175780) is a neurological disorder characterized by fluid-filled cysts or cavities in the brain.[1] It has been suggested that porencephalic cysts are caused by a disturbance of vascular supply leading to cerebral degeneration.[2,3] Porencephaly clinically causes hemiplegia (most often), tetraplegia, epilepsy, and intellectual disability.[4,5] Monozygous twinning, maternal cardiac arrest or abdominal trauma, a deficient protein C anticoagulant pathway, or cytomegalovirus infections are risk factors for sporadic porencephaly.[2,6] Recently, mutations in the gene encoding type IV collagen α1 chain (*COL4A1* [MIM 120130]) have been shown to cause familial porencephaly.[7] Since then, de novo and inherited *COL4A1* mutations have been reported,[8–10] confirming that *COL4A1* abnormalities are involved in both sporadic and familial porencephaly. Type IV collagens are basement membrane proteins that are expressed in all tissues including the vasculature. COL4A1 (α1 chain) and COL4A2 (α2 chain) are the most abundant type IV collagens, and form heterotrimers with 2:1 stoichiometry (α1α1α2).[11] A mouse model of the heterozygous *COL4A1* mutation (*Col4a1*$^{+/\Delta ex40}$) showed cerebral hemorrhage and porencephaly and displayed abnormalities of vascular basement membranes, such as uneven edges, inconsistent density, and highly variable thickness.[7] In addition, a dominant negative effect of the *Col4a1*$^{+/\Delta ex40}$ mutation was demonstrated on collagen IV α1α1α2 heterotrimer assembly and its secretion.[7] In humans, most mutations are substitutions of the conserved Gly residue in the Gly-Xaa-Yaa repeat of the triple-helical domain, and they have a dominant negative effect on heterotrimer formation.[11,12]

COL4A2 (MIM 120090), which encodes the type IV α2 collagen chain, is a possible candidate for porencephaly because its mutations may affect the α1α1α2 heterotrimer. Supporting this idea, osteogenesis imperfecta type I-IV (MIM 166200, 166210, 259420, and 166220), which is characterized by abnormal bone fragility and low bone mass, is caused by mutations in both *COL1A1* (MIM 120150) and *COL1A2* (MIM 120160) that may interfere with formation of the collagen I α1α1α2 heterotrimer.[13] Moreover, mice lines harboring *Col4a2* point mutations (*Col4a2*^{ENU415}, c.227G>T [p.Val31Phe]; *Col4a2*^{ENU4003} and *Col4a2*^{ENU4020}, c.2073G>A [p.Gly646Asp]) showed abnormalities of the lens, cornea, and vascular stability.[14] In the brains of the mutants, pseudocysts in the upper cortical plate, hemorrhages surrounding small blood vessels, and focal hemorrhagic necroses were observed, indicating that *Col4a2* mutations cause abnormalities of the cerebral vasculature similar to those caused by *Col4a1* mutations.[7,14] In this study, we screened for *COL4A2* mutations in 35 Japanese individuals with porencephaly. Substitutions of a Gly residue in the Gly-Xaa-Yaa repeat were identified in two individuals (individuals 1 and 2). Clinical information and peripheral blood samples were

[1]Department of Human Genetics, Yokohama City University Graduate School of Medicine, Fukuura 3-9, Kanazawa-ku, Yokohama 236-0004, Japan; [2]Department of Pediatrics, Tohoku University School of Medicine, Seiryo-machi 1-1, Aoba-ku, Sendai 980-8574, Japan; [3]Department of Pediatric Neurology, Takuto Rehabilitation Center for Children, Akiu-machi 20, Taihaku-ku, Sendai 982-0241, Japan; [4]Department of Pediatric Neurology, Morinomiya Hospital, Morinomiya2-1-88, Joto-ku, Osaka 536-0025, Japan; [5]Department of Neonatal Medicine and Pediatrics, Osaka Medical College, 2-7 Daigakumachi, Takatsuki, Osaka 569-8686, Japan; [6]Department of Pediatric Neurology, Seirei-Mikatahara General Hospital, 2-12-12 Sumiyoshi, Naka-ku, Hamamatsu 430-8558, Japan; [7]Division of Neurology, Clinical Research Institute, Kanagawa Children's Medical Center, 2-138-4 Mutsukawa, Minami-ku, Yokohama 232-8555, Japan; [8]Department of Pediatrics, Yamagata University School of Medicine, Iida-nishi 2-2-2, Yamagata 990-9585, Japan
*Correspondence: hsaitsu@yokohama-cu.ac.jp
DOI 10.1016/j.ajhg.2011.11.016.

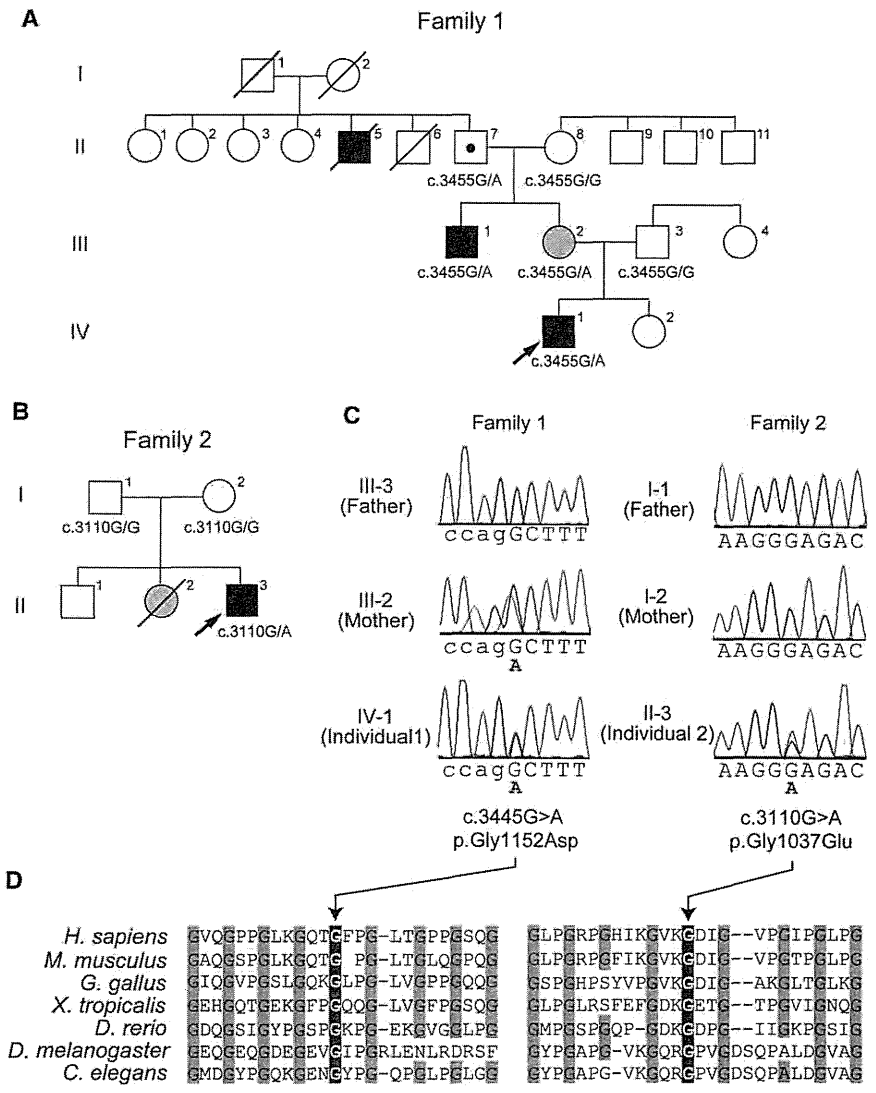

Figure 1. Pedigrees and *COL4A2* Mutations in Individuals 1 and 2

Pedigrees of family 1(A) and family 2 (B). The arrows indicate the probands (Individual 1 in family 1 and individual 2 in family 2). The segregation of the *COL4A2* mutations is shown. In family 1, the proband's mother (III-2) and maternal uncle (III-1) had mild monoparesis of the left upper extremity and congenital left hemiplegia and an assisted walk, respectively. The maternal grandfather (II-7) was healthy. The elder granduncle (II-5) was also afflicted by congenital hemiplegia and died in his 60s. (B) In family 2, the proband had a heterozygous mutation, but his parents did not have this mutation, indicating that the mutation occurred de novo. His elder sister (II-2) had intraventricular hemorrhage two days after birth but her DNA was unavailable.

(C) Electropherogram of family 1 (left) and family 2 (right). The intron and exon bases are in lower and upper cases, respectively. The c.3455G>A (p.Gly1152Asp) mutation in individual 1 was inherited from his mother. The c.3110G>A (p.Gly1037Glu) mutation in individual 2 occurred de novo.

(D) Multiple amino acid sequence alignments of COL4A2 proteins showing the evolutionarily conserved amino acids. The protein sequences obtained from the National Center for Biotechnology Information protein database are, NP_001837.2 (*Homo sapiens*), NP_034062.3 (*Mus musculus*), NP_001155862.1 (*Gallus gallus*), XP_002933063.1 (*Xenopus tropicalis*), XP_687811.5 (*Danio rerio*), AAB64082.1 (*Drosophila melanogaster*), and CAA80537.1 (*Caenorhabditis elegans*). The multiple sequence alignment was performed via the CLUSTALW website (see Web Resources). The positions of the conserved Gly residues in the Gly-X-Y repeats where the mutations occurred are highlighted with gray.

obtained from their family members after obtaining written informed consent. Experimental protocols were approved by the Institutional Review Board of Yokohama City University School of Medicine.

Individual 1 is 7 years old and a product of nonconsanguineous healthy parents (Figure 1A, arrow). There was no abdominal traumatism associated with the pregnancy and delivery in the mother. The individual was born at 36 weeks' gestation with a planned Caesarean section because, at 31 weeks' gestation, an antenatal ultrasound scan revealed an enlarged right lateral ventricle. Apgar scores were 9 at 1 min and 10 at 5 min. He weighed 2,900 g (+1.09 standard deviation [SD]) and had a head circumference of 32.5 cm (+0.05 SD). His early development was delayed with poor left hand use and abnormal leg movement. Brain magnetic resonance imaging (MRI) at 6 months showed an enlarged right lateral ventricle. Abrupt vomiting and nausea followed by motionless arrest developed at the 10 months. An electroencephalogram (EEG) showed focal spikes in the right frontal region, and carbamazepine treatment was initiated at the 12 months. Rehabilitation was started at 10 months. The individual started rolling at 12 months, crawling at 18 months, and walking alone at 3 years. He had spastic triplegia (diplegia and left hemiplegia) showing hemiplegic and diplegic gait with fluent speech and normal word comprehension. At the 5 years of age, he underwent orthopedic surgery for foot deformity due to spastic paresis. An EEG showed spikes in the right occipital to posterior temporal region and midcentral region. A brain MRI at age 6 showed an enlarged right lateral ventricle, reduced volume of the right frontal white matter, and atrophic right cerebral peduncle and body of corpus callosum (Figures 2A–2C). His intelligent quotient [IQ] score, evaluated at 6 years with Wechsler Intelligence Scale for Children-Third Edition (WISC-III), was 74 (his performance IQ was 69 and his verbal IQ was

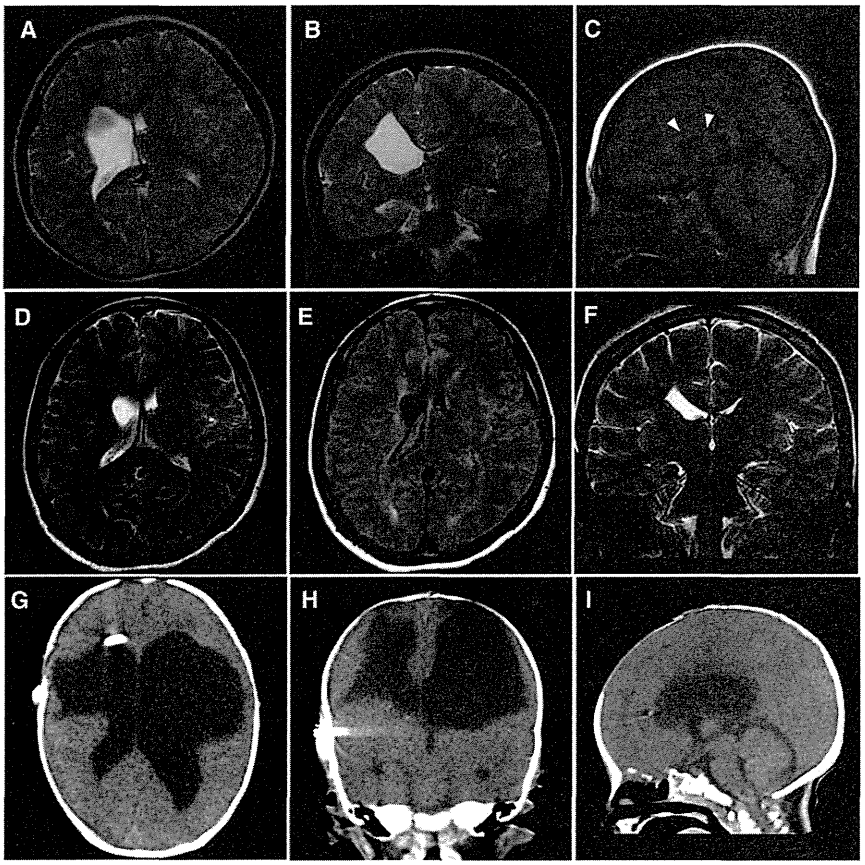

Figure 2. Brain Imaging in Individuals 1 and 2

(A–C) Brain MRIs of individual 1 at 6 years old; (A) T2-weighted axial image. (B) Coronal image. The images in (A) and (B) show an enlarged right lateral ventricle and a reduced volume of the right frontal white matter. (C) T1-weighted midline sagittal image showing atrophy of the body of the corpus callosum (arrowheads). The lesion responsible for the left leg paresis is not evident in these images.

(D–F) Brain MRIs of individual 1's mother at age 31. (D) T2-weighted axial and (F) coronal images show a mildly enlarged right lateral ventricle. (E) FLAIR axial image shows high signal intensity around the enlarged ventricular wall, which is consistent with mild porencephaly or periventricular venous infarction.

(G–I) CT images of individual 2 at 2 months of age. (G) Axial image. (H) Coronal image. (I) Sagittal image. The images in (G), (H), and (I) show an enlarged bilateral lateral ventricle and an extremely reduced volume of bilateral frontal white matter. The V-P shunt tube is also visible in the right lateral ventricle. The pontocerebellar structures seem to be normal.

82). The individual is now 7 years old and attending a local school. He can walk with ankle foot orthosis and hand assist. The epilepsy is well controlled with carbamazepine and clobazam. He does not show hematuria, muscular cramps, or ophthalmic abnormalities. His mother was born at term without asphyxia after an uneventful pregnancy. She had convulsions at the age of 18 months, and anticonvulsant was started under a diagnosis of focal epilepsy. Seizures were well controlled and treatment was discontinued at the age of 13. She first realized clumsiness of the left hand when she started learning piano and recorder at the age of 9. When she was a junior high school student, she felt severe headaches, and abnormal findings were pointed out in the brain MRI study (detailed information was unavailable). However, she did not undergo any more examinations because the headaches disappeared and did not recur. Neurological examination at 31 years revealed very mild monoparesis of the left upper extremity. She had neither spasticity nor exaggerated tendon reflexes. The grip power of her right and left hands was 25 and 15 kg, respectively. Mirror movement was observed on the right hand. The brain MRI revealed a mildly enlarged right lateral ventricle and high signal intensity around the enlarged ventricular wall on a Fluid Attenuated Inversion Recovery (FLAIR) image, which is consistent with mild porencephaly or periventricular venous infarction (Figures 2D–2F). MR angiography showed no aneurysms. Of note, his maternal elder uncle also showed congenital left hemiplegia with an assisted walk, and his maternal granduncle had also been afflicted by congenital hemiplegia, suggesting a genetic predisposition in the family (Figure 1A).

Individual 2 is 1 year and 4 months old and a product of nonconsanguineous healthy parents (Figure 1B, arrow). There was no abdominal traumatism associated with the pregnancy and delivery in the mother. He was born at 35 weeks' gestation. His birth weight was 1,694 g (−2.36 SD) and his head circumference was 29 cm (−1.77 SD). Mild asphyxia was observed, and he had Apgar scores of 3 at 1 min and 7 at 5 min. An ultrasound scan at 6 hr after birth revealed a parenchymal hemorrhage of the right cerebral hemisphere with an enlarged left lateral ventricle. Because a blood test revealed significant increases in prothrombin time (29.3 s) and activated partial thromboplastin time (104.3 s), but not in D-dimer (0.7 μg/ml) at 1 day after birth, he was treated with a daily infusion of fresh frozen plasma for 12 days. At 37 days after birth, he underwent a ventricular-peritoneal shunt (V-P shunt) operation for progressive enlargement of the lateral ventricle. Computed tomography (CT) at 2 months of age showed an enlarged bilateral lateral ventricle and an extremely reduced volume of bilateral frontal white matter (Figures 2G–2I). Blood coagulation was normalized at 7 months. At the 7 months, the individual did not show any head control or rolling, and presented with abnormal posturing and spastic quadriplegia dominant on the left side of his body. With

rehabilitation, he had full-range visual pursuit, a social smile, and incomplete head control. Although his spasticity improved, exaggerated deep tendon reflexes with synergic voluntary movement of the distal part of the extremities were recognized. An EEG at 1 year of age showed no epileptic discharges. His present developmental quotient is below 20. He did not show hematuria, muscular cramps, intracranial aneurysms, or cataracts. His elder sister was found to have an intraventricular hemorrhage two days after birth and underwent a V-P shunt. Her development was almost normal, and internal strabismus was noted. Unfortunately, she died in an accident at the age of four, and so her DNA was unavailable (Figure 1B).

Genomic DNA was isolated from peripheral blood leukocytes according to standard methods. DNA for mutation screening was amplified by illustra GenomiPhi V2 DNA Amplification Kit (GE Healthcare, Buckinghamshire, UK). The DNA of family members of individual 1 was isolated from saliva samples with Oragene (DNA Genotek Inc., Ontario, Canada). Exons 2 to 48 covering the entire *COL4A2* coding region (GenBank accession number NM_001846.2) were examined by high-resolution melting curve (HRM) analysis or directly sequenced (for exon 46). The samples showing an aberrant melting curve pattern in the HRM analysis were sequenced. PCR primers and conditions are shown in Table S1, available online. All the mutations were verified with genomic DNA as a template. Two heterozygous mutations, c.3455G>A (p.Gly1152Asp) in individual 1 and c.3110G>A (p.Gly1037Glu) in individual 2, were identified. Both mutations occur at evolutionary conserved Gly residues in the Gly-X-Y repeats (Figure 1D), suggesting that the two mutations may alter the collagen IV $\alpha1\alpha1\alpha2$ heterotrimers. These mutations were absent in 200 normal Japanese controls, and our evaluation with web-based prediction tools strongly suggested that these substitutions are pathogenic (Table S2). Screening for *COL4A1* mutations was negative for both individuals (data not shown). The c.3455G>A mutation was found in the proband's mother and the maternal uncle, who showed very mild monoparesis of the left upper extremity and congenital left hemiplegia, respectively, and in maternal grandfather who is asymptomatic (Figures 1A and 1B). Therefore the c.3455G>A mutation can be considered as a pathogenic mutation with incomplete penetrance. The c.3110G>A mutation in individual 2 was not found in his parents, indicating that this mutation occurred de novo (Figure 1C).

Here we report two individuals with porencephaly who harbor *COL4A2* mutations. In individual 2, the mutation occurred de novo. It is noteworthy that individual 2's elder sister also suffered from an intraventricular hemorrhage. A coincidental phenocopy in the sister is possible and would be consistent with de novo occurrence of the mutation. Alternatively, the sister might have the same mutation, which could be inherited from either one of the parents with a germline-mosaic mutation, though it was impossible to examine the sister because her sample is unavailable. Thus, with the present data, we concluded that the c.3110G>A mutation occurred de novo. On the other hand, the mutation in individual 1 was inherited from his mildly affected mother. In addition, congenital hemiplegia is observed in familial members of individual 1; the segregation of the c.3455G>A mutation is consistent with a dominant trait with incomplete penetrance. Such incomplete penetrance also has been reported in familial porencephalies with *COL4A1* mutations,[8,9] suggesting that abnormalities of collagen IV $\alpha1\alpha1\alpha2$ heterotrimers may conspire with other risk factors. The porencephalic cyst was unilateral in individual 1 and bilateral in individual 2, who required shunting, indicating variable severities caused by the different *COL4A2* mutations. Most porencephalic cysts caused by *COL4A1* mutations are unilateral;[9] however, Meuwissen et al. recently reported *de novo COL4A1* mutations in sporadic extensive bilateral porencephaly resembling hydranencephaly, indicating similar variable severities caused by *COL4A1* mutations.[10] Thus the involvement of *COL4A1* and *COL4A2* abnormalities should be considered in porencephaly and related pre- and perinatal cerebral hemorrhages, regardless of their severities.

It has been reported that *COL4A1* mutations cause a variety of phenotypes, including porencephaly, infantile hemiplegia, and cerebral small vessel diseases involving both ischemic stroke and intracerebral hemorrhage with radiological features of lacunar infarction, and leukoaraiosis in adult individuals.[9,15–18] The phenotypes in the central nervous system are often accompanied by ocular features (cataracts, retinal vessel tortuosity and hemorrhage, and defects of the anterior segment of the eye), nephropathy, and muscle cramps.[9,16,17] Considering the common pathological mechanism between *COL4A1* and *COL4A2* mutations (abnormalities of collagen IV $\alpha1\alpha1\alpha2$ heterotrimers), *COL4A2* mutations also may be involved in small vessel diseases that can be manifested in adulthood. Supporting this idea, mice lines harboring *Col4A2* point mutations showed cataracts, abnormalities of the lens and the cornea, and cerebral abnormalities.[14] Thus it is important to identify mutations in both *COL4A1* and *COL4A2* in individuals with porencephaly as well as in asymptomatic carriers, for whom the prevention of stroke and genetic counseling are quite important. Identification of pathogenic mutations in individuals with porencephaly is of great interest for obstetricians and pediatricians, and for neurologists working for adult individuals.

In summary, we have identified mutations in *COL4A2* as a genetic cause of both sporadic and familial porencephaly. Our data further support the importance of genetic testing in porencephaly and related pre- and perinatal cerebral hemorrhages for which the genetic predisposition is gradually being uncovered.

Supplemental Data

Supplemental Data include two tables and can be found with this article online at http://www.cell.com/AJHG/.

Acknowledgments

We would like to thank all the individuals and their families for their participation in this study. This work was supported by research grants from the Ministry of Health, Labour and Welfare (K.H., N. Miyake, H.O., M.K., N. Matsumoto, and H.S.), the Japan Science and Technology Agency (N. Matsumoto), the Strategic Research Program for Brain Sciences (N. Matsumoto), and a Grant-in-Aid for Scientific Research on Innovative Areas-(Foundation of Synapse and Neurocircuit Pathology)-from the Ministry of Education, Culture, Sports, Science and Technology of Japan (N. Matsumoto), a Grant-in-Aid for Scientific Research from Japan Society for the Promotion of Science (H.O., N. Matsumoto), a Grant-in-Aid for Young Scientist from Japan Society for the Promotion of Science (H.D., N. Miyake, H.S.) and a grant from the Takeda Science Foundation (N. Miyake and N. Matsumoto). This work has been done at the Advanced Medical Research Center, Yokohama City University, Japan.

Received: September 27, 2011
Revised: November 4, 2011
Accepted: November 17, 2011
Published online: December 29, 2011

Web Resources

The URLs for data presented herein are as follows:

Clustal W, http://www.genome.jp/tools/clustalw/
GenBank, http://www.ncbi.nlm.nih.gov/Genbank/
Online Mendelian Inheritance in Man (OMIM), http://www.omim.org

References

1. Berg, R.A., Aleck, K.A., and Kaplan, A.M. (1983). Familial porencephaly. Arch. Neurol. *40*, 567–569.
2. Govaert, P. (2009). Prenatal stroke. Semin. Fetal Neonatal Med. *14*, 250–266.
3. Hunter, A. (2006). Porencephaly. In Human Malformations and related Anomalies, S. Re and H. Jg, eds. (New York: Oxford University Press), pp. 645–654.
4. Mancini, G.M., de Coo, I.F., Lequin, M.H., and Arts, W.F. (2004). Hereditary porencephaly: clinical and MRI findings in two Dutch families. Eur. J. Paediatr. Neurol. *8*, 45–54.
5. Vilain, C., Van Regemorter, N., Verloes, A., David, P., and Van Bogaert, P. (2002). Neuroimaging fails to identify asymptomatic carriers of familial porencephaly. Am. J. Med. Genet. *112*, 198–202.
6. Moinuddin, A., McKinstry, R.C., Martin, K.A., and Neil, J.J. (2003). Intracranial hemorrhage progressing to porencephaly as a result of congenitally acquired cytomegalovirus infection—an illustrative report. Prenat. Diagn. *23*, 797–800.
7. Gould, D.B., Phalan, F.C., Breedveld, G.J., van Mil, S.E., Smith, R.S., Schimenti, J.C., Aguglia, U., van der Knaap, M.S., Heutink, P., and John, S.W. (2005). Mutations in *Col4a1* cause perinatal cerebral hemorrhage and porencephaly. Science *308*, 1167–1171.
8. Breedveld, G., de Coo, I.F., Lequin, M.H., Arts, W.F., Heutink, P., Gould, D.B., John, S.W., Oostra, B., and Mancini, G.M. (2006). Novel mutations in three families confirm a major role of *COL4A1* in hereditary porencephaly. J. Med. Genet. *43*, 490–495.
9. Lanfranconi, S., and Markus, H.S. (2010). *COL4A1* mutations as a monogenic cause of cerebral small vessel disease: a systematic review. Stroke *41*, e513–e518.
10. Meuwissen, M.E., de Vries, L.S., Verbeek, H.A., Lequin, M.H., Govaert, P.P., Schot, R., Cowan, F.M., Hennekam, R., Rizzu, P., Verheijen, F.W., et al. (2011). Sporadic *COL4A1* mutations with extensive prenatal porencephaly resembling hydranencephaly. Neurology *76*, 844–846.
11. Khoshnoodi, J., Pedchenko, V., and Hudson, B.G. (2008). Mammalian collagen IV. Microsc. Res. Tech. *71*, 357–370.
12. Engel, J., and Prockop, D.J. (1991). The zipper-like folding of collagen triple helices and the effects of mutations that disrupt the zipper. Annu. Rev. Biophys. Biophys. Chem. *20*, 137–152.
13. Gajko-Galicka, A. (2002). Mutations in type I collagen genes resulting in osteogenesis imperfecta in humans. Acta Biochim. Pol. *49*, 433–441.
14. Favor, J., Gloeckner, C.J., Janik, D., Klempt, M., Neuhäuser-Klaus, A., Pretsch, W., Schmahl, W., and Quintanilla-Fend, L. (2007). Type IV procollagen missense mutations associated with defects of the eye, vascular stability, the brain, kidney function and embryonic or postnatal viability in the mouse, Mus musculus: an extension of the *Col4a1* allelic series and the identification of the first two *Col4a2* mutant alleles. Genetics *175*, 725–736.
15. Vahedi, K., and Alamowitch, S. (2011). Clinical spectrum of type IV collagen (COL4A1) mutations: a novel genetic multisystem disease. Curr. Opin. Neurol. *24*, 63–68.
16. Sibon, I., Coupry, I., Menegon, P., Bouchet, J.P., Gorry, P., Burgelin, I., Calvas, P., Orignac, I., Dousset, V., Lacombe, D., et al. (2007). *COL4A1* mutation in Axenfeld-Rieger anomaly with leukoencephalopathy and stroke. Ann. Neurol. *62*, 177–184.
17. Alamowitch, S., Plaisier, E., Favrole, P., Prost, C., Chen, Z., Van Agtmael, T., Marro, B., and Ronco, P. (2009). Cerebrovascular disease related to *COL4A1* mutations in HANAC syndrome. Neurology *73*, 1873–1882.
18. Gould, D.B., Phalan, F.C., van Mil, S.E., Sundberg, J.P., Vahedi, K., Massin, P., Bousser, M.G., Heutink, P., Miner, J.H., Tournier-Lasserve, E., and John, S.W. (2006). Role of COL4A1 in small-vessel disease and hemorrhagic stroke. N. Engl. J. Med. *354*, 1489–1496.

Journal of Child Neurology
27(2) 218-221

DOI: 10.1177/0883073811416239
http://jcn.sagepub.com
SAGE

Congenital Dysplastic Microcephaly and Hypoplasia of the Brainstem and Cerebellum With Diffuse Intracranial Calcification

Kazuyuki Nakamura, MD, Mitsuhiro Kato, MD, PhD, Ayako Sasaki, MD, PhD, Masayo Kanai, MD, PhD, and Kiyoshi Hayasaka, MD, PhD

Abstract

Congenital microcephaly with intracranial calcification is a rare condition presented in heterogeneous diseases. Here, we report the case of a 1-year-old boy with severe congenital microcephaly and diffuse calcification. Neuroimaging studies showed a diffuse simplified gyral pattern; a very thin cortex; ventricular dilatation; very small basal ganglia, thalamus, and brainstem; and cerebellar hypoplasia with diffuse calcification. Clinical features of intrauterine infections, such as neonatal jaundice, hepatomegaly, and thrombocytopenia, were not found. Serological tests, cultures, and polymerase chain reaction analysis were negative for viral infections. The etiology of pseudo–toxoplasmosis, rubella, cytomegalovirus, and herpes simplex syndrome is still unknown. This study describes the most severe form of pseudo–toxoplasmosis, rubella, cytomegalovirus, and herpes simplex syndrome reported to date, with the patient showing microcephaly and calcification or band-like intracranial calcification with simplified gyration and polymirogyria.

Keywords

microcephaly, intracranial calcification, pontocerebellar hypoplasia, toxoplasmosis, rubella, cytomegalovirus, herpes simplex

Received February 23, 2011. Accepted for publication June 16, 2011.

Congenital microcephaly with brain dysgenesis and intracranial calcification is a characteristic feature of intrauterine infections of toxoplasma, rubella, cytomegalovirus, herpes virus, and other infectious agents, including human immunodeficiency virus and the bacteria that cause syphilis. This form of congenital microcephaly has been termed the toxoplasmosis, rubella, cytomegalovirus, and herpes simplex syndrome.[1] In addition to congenital microcephaly and intracranial calcification, toxoplasmosis, rubella, cytomegalovirus, and herpes simplex syndrome shows systemic abnormalities, such as thrombocytopenia, anemia, hepatosplenomegaly, liver dysfunction, jaundice, and chorioretinitis, with elevated serum immunoglobulin M (IgM) levels at birth. Similar clinical conditions have been reported in several patients with familial occurrence but with no evidence of infection. These clinical conditions have been designated as "pseudo–toxoplasmosis, rubella, cytomegalovirus, and herpes simplex" syndrome.[2] In addition, "band-like intracranial calcification with simplified gyration and polymicrogyria" has also been reported. However, this syndrome shows no evidence of infection, abnormalities in liver function, or thrombocytopenia.[3,4]

It is important to discriminate these syndromes for genetic counseling. This report describes a patient with congenital microcephaly and whole brain dysgenesis and extensive calcification, suggesting a severe form of pseudo–toxoplasmosis, rubella, cytomegalovirus, and herpes simplex syndrome, or band-like intracranial calcification with simplified gyration and polymicrogyria.

Case Report

The boy was born to healthy, unrelated, 29-year-old Japanese parents. This was the mother's first pregnancy, and the boy had no siblings. There were no household pets including cats. During the 5- to 6-week period of gestation, his mother had fever for 1 day but showed no other symptoms. Microcephaly was first observed on ultrasound examination conducted at 28 weeks of gestation. At 34 weeks of gestation, specific IgMs

Department of Pediatrics, Yamagata University Faculty of Medicine, Yamagata, Japan

Corresponding Author:
Kazuyuki Nakamura, MD, Department of Pediatrics, Yamagata University Faculty of Medicine, 2-2-2, Iida-Nishi, Yamagata 990-9585, Japan
Email: kazun-yamagata@umin.ac.jp

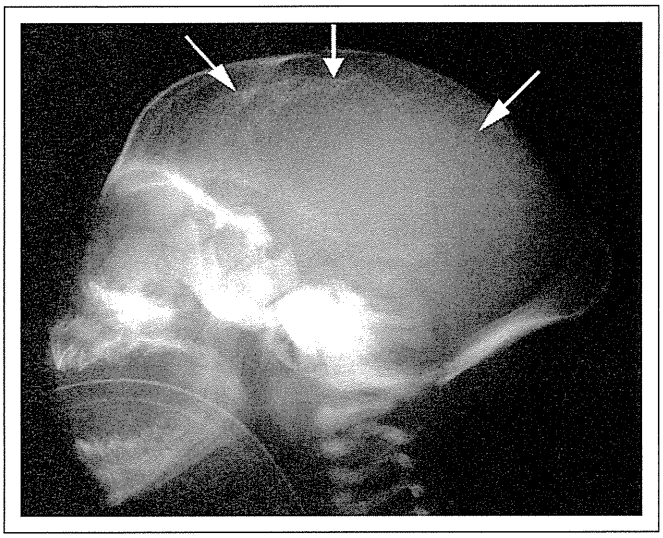

Figure 1. A plain radiograph of the head shows the cranial vault with a frontal sloping and a marked external occipital protuberance. Intracranial high-density spots are visible along the cerebral wall (arrows).

against rubella, cytomegalovirus, and toxoplasma were negative in the mother. He was delivered by caesarean section because of hypotonic uterine dysfunction at 42 weeks of gestation. His Apgar score was 1 at 1 min. He required intratracheal intubation for severe dyspnea. His weight at birth was 3140 g; length, 46 cm (−2.0 SD); and head circumference, 29 cm (−3.2 SD). He had bilateral undescended testis without hepatosplenomegaly or a petechial rash. Ophthalmologic examination showed no corneal clouding or chorioretinitis. Neurological examination showed the presence of hypotonic muscles and absence of a Moro reflex. Skull radiography showed a sloping forehead and several intracranial calcific densities (Fig. 1). A computed tomographic (CT) scan of the head showed prominent calcification mainly along the ventricular wall from the cerebrum to the brain stem (Fig. 2). Magnetic resonance imaging (MRI) of the brain showed severe diffuse simplified gyri combined with a thinning of the cortex and the white matter; marked dilated ventricles; and severe hypoplasia of the basal ganglia, thalamus, cerebellum, and brainstem (Fig. 3). At the age of 4 days, a hematological examination (hemoglobin, 18.3 g/dL; white blood cells, 10 010/μL; neutrophils, 69%; platelets, 32.8 $\times$ $10^4/\mu L^3$) and blood chemistry tests, including those for calcium, phosphate, aspartate aminotransferase, alanine aminotransferase, lactate, and amino acids were normal. The total serum IgM was 8 mg/dL; the specific IgMs against toxoplasma, rubella, cytomegalovirus, herpes simplex, and varicella-zoster virus were negative. Viral cultures of a pharyngeal swab and urine were negative. Subsequent polymerase chain reaction (PCR) amplification of cytomegalovirus DNA in urine and the umbilical cord was also negative. An antibody titer for lymphocytic choriomeningitis virus was negative. G-banding chromosomal analysis showed a karyotype of 46, XY. At the age of 10 months, a cerebrospinal fluid examination did not show increased number of lymphocytes or interferon-alpha.

Figure 2. Computed tomographic scan of the head shows linear or patchy high signals consisting of calcifications within or immediately beneath the cortex and the enlargement of the lateral ventricles.

Electroencephalography showed multifocal sharp waves with low-voltage background activity. At 12 months of age, he showed hypothermia (<36°C); recurrent urinary tract infections caused by vesicoureteral reflux; and a profound developmental delay with limb contractures, no eye contact, and no head control. He received tube feeding because of bulbar palsy.

Discussion

Congenital microcephaly results from various clinical conditions such as infections, radiation, exogenous toxic agents, anoxic or metabolic insults, and genetic bases.[1] Although these conditions can also cause cerebral calcification, the association of congenital microcephaly and calcification are rare. Our patient experienced a febrile episode, suggesting an infection at 5 to 6 weeks of gestation, but there was no history of any other insult. Since intrauterine infections or toxoplasmosis, rubella, cytomegalovirus, and herpes simplex syndrome, especially cytomegalovirus infection, is the most frequent cause of congenital microcephaly and since calcification and earlier infection induce severer brain anomalies,[1] we tried to obtain evidence of a prenatal infection of cytomegalovirus using serological tests, cultures, and PCR amplification. However, none of these tests yielded a positive result, which could be a result of early infection during fetal development. The fetus showed no immunological response, and the virus could not be cultured. Moreover, the PCR sensitivity was sufficiently high enough to detect viral DNA.[5] On

Figure 3. Sagittal T2-weighted magnetic resonance imaging (MRI) shows a thin cortex and white matter with an undetectable border. Prominent hypoplasia of the cerebellum and brainstem is visible.

the basis of these results, we conclude that cytomegalovirus is unlikely to be the cause of our patient's condition.

During the middle embryonic period (5–6 weeks of gestation in humans), secondary brain vesicles (telencephalon, diencephalon, mesencephalon, metencephalon, and myelencephalon) are formed; the primitive cerebral hemispheres develop during neuronogenesis in the ventricular zone. Insult at this stage can engender extremely severe brain malformation (eg, decreased brain size) because of the inhibition of cell proliferation and the dysplastic configuration of the brain that results from impaired cell migration. The hypoplastic brainstem and cerebellum as well as microcephaly with the thin cortex and irregular convolution seen in our patient suggest an event during early embryogenesis, although the etiology is unknown.

Although our patient showed an irregular convolution that suggested possible cortical dysplasia, the very thin cortex suggested microcephaly with normal to thin cortex or microcephaly with a simplified gyral pattern.[6] To date, 5 genes (*MCPH1, ASPM, CDK5RAP2, CENPJ,* and *SLC25A19*) have been found to be responsible for the autosomal recessive inheritance of microcephaly with a simplified gyral pattern.[7,8] Mutations in these genes result in congenital microcephaly but not in a calcification resembling the one in our patient. Microcephaly with polymicrogyria or other cortical dysplasias or microcephaly with pontocerebellar hypoplasia are other candidate conditions for our patient, but neither one shows calcification.[9] At this point, it is difficult to categorize the neuroimaging features of our patient into the classification scheme for malformations of cortical development.[6]

Aicardi–Goutières syndrome is an autosomal recessive form of progressive encephalopathy characterized by acquired microcephaly, leukodystrophy, and calcifications of the basal ganglia, which is similar to toxoplasmosis, rubella, cytomegalovirus, and herpes simplex syndrome.[10] Recently, 5 genes (*TREX1, RNASEH2B, RNASEH2C, RNASEH2A,* and *SAMHD1*) have been identified as the responsible genes for this syndrome.[11-13] Elevated interferon-alpha levels and chronic lymphocytosis in the cerebrospinal fluid are specific features of Aicardi–Goutières syndrome. However, our patient had neither of these features. Although cerebrospinal fluid lymphocytosis is not necessary for an Aicardi–Goutières syndrome diagnosis[14] and although a small number of patients show microcephaly at birth, the cerebral dysplasia observed in our patient has never been reported as a manifestation of Aicardi–Goutières syndrome.

It has been suggested that pseudo–toxoplasmosis, rubella, cytomegalovirus, and herpes simplex syndrome is the same disorder as Aicardi–Goutières syndrome.[15] Periventricular areas are commonly calcified in pseudo–toxoplasmosis, rubella, cytomegalovirus, and herpes simplex syndrome, but the basal ganglia, cerebellum, and brainstem can also be affected. Brain MRIs often show cerebral atrophy, enlarged lateral ventricles, and severe hypoplasia of the corpus callosum, cerebellum, and brainstem. Some patients also show associated cortical dysplasia.[2,16] One report described a patient as having microcephaly with plate-like cortical calcification and with an extremely decreased convolution of the cerebral cortex, which is similar to our patient's condition.[17] However, the brainstem and cerebellum were spared in that patient.

Band-like intracranial calcification with simplified gyration and polymicrogyria is inherited as an autosomal recessive trait, and mutations of the *OCLN* gene have been identified as resulting in this condition.[18] Band-like intracranial calcification with simplified gyration and polymicrogyria is similar to pseudo–toxoplasmosis, rubella, cytomegalovirus, and herpes simplex syndrome in that both show widespread intracranial calcification and polymicrogyria and that some patients show hypoplasia of the cerebellum and brainstem. There are differences between these 2 conditions in terms of the postnatal microcephaly, the characteristic band-like calcification, and the lack of evidence for neonatal disturbance of liver function with thrombocytopenia; nonetheless, they can have similar etiologies.[3,4]

The extensive lesions of the brain are reminiscent of multicystic encephalomalacia, which are often accompanied by extensive dystrophic calcifications in zones of infarction. Multicystic encephalomalacia is also caused by fetal viral infection as well as hypoxia or circulatory insults; however, the lesions in the patient appeared to be too broad for secondary injury and had no visible cysts, as observed by MRI. The size and number of cysts depends on the stage of infarction, which can be both of major cerebral vessels and of the microcirculation at capillary levels.[19] Neuropathological confirmation is essential to reveal the pathogenesis.

It is noteworthy that this is the most severe case of a patient with congenital dysplastic microcephaly and brainstem and cerebellar hypoplasia with extensive intracranial calcification. The pathogenesis, particularly regarding its inheritance, remains to be clarified.

Acknowledgments

The authors thank Dr William B. Dobyns of the University of Chicago for his valuable comments and Dr Keiko Ishii, Tohoku University, for examining cytomegalovirus infection.

Author Contributions

KN contributed in organizing the article and wrote the first draft of the manuscript. M. Kato and KH performed a review and critique of the manuscript. KN, M. Kato, AS, and M. Kanai primarily managed the patient.

Declaration of Conflicting Interests

The authors declared no potential conflicts of interest with respect to the research, authorship, and/or publication of this article.

Funding

The authors received no financial support for the research, authorship, and/or publication of this article.

Ethical Approval

The authors received an informed consent form from the parents of the patient.

References

1. Volpe JJ. In: *Neurology of the Newborn*. 5th ed. Philadelphia, PA: WB Saunders;; 2008.
2. Vivarelli R, Grosso S, Cioni M, et al. Pseudo-TORCH syndrome or Baraitser-Reardon syndrome: diagnostic criteria. *Brain Dev*. 2001;23:18-23.
3. Briggs TA, Wolf NI, D'Arrigo S, et al. Band-like intracranial calcification with simplified gyration and polymicrogyria: a distinct "pseudo-TORCH" phenotype. *Am J Med Genet A*. 2008;146: 3173-3180.
4. Abdel-Salam GM, Zaki MS, Saleem SN, Gaber KR. Microcephaly, malformation of brain development and intracranial calcification in sibs: pseudo-TORCH or a new syndrome. *Am J Med Genet A*. 2008;146:2929-2936.
5. Revello MG, Zavattoni M, Furione M, et al. Diagnosis and outcome of preconceptional and periconceptional primary human cytomegalovirus infections. *J Infect Dis*. 2002;186:553-557.
6. Barkovich AJ, Kuzniecky RI, Jackson GD, et al. A development and genetic classification for malformations of cortical development. *Neurology*. 2005;65:1873-1887.
7. Rosenberg MJ, Agarwala R, Bouffard G, et al. Mutant deoxynucleotide carrier is associated with congenital microcephaly. *Nat Genet*. 2002;32:175-179.
8. Woods CG, Bond J, Enard W. Autosomal recessive primary microcephaly (MCPH): a review of clinical, molecular, evolutionary findings. *Am J Hum Genet*. 2005;76:717-728.
9. Hashimoto K, Takeuchi Y, Kida Y, et al. Three siblings of fatal infantile encephalopathy with olivopontocerebellar hypoplasia and microcephaly. *Brain Dev*. 1998;20:169-174.
10. Goutières F. Aicardi-Goutières syndrome. *Brain Dev*. 2005;27: 201-206.
11. Crow YJ, Leitch A, Hayward BE, et al. Mutations in genes encoding ribonuclease H2 subunits cause Aicardi-Goutières syndrome and mimic congenital viral brain infection. *Nat Genet*. 2006;38: 910-916.
12. Crow YJ, Hayward BE, Parmar R, et al. Mutations in the gene encoding the 3'-5' DNA exonuclease TREX1 cause Aicardi–Goutières syndrome at the AGS1 locus. *Nat Genet*. 2006;38: 917-920.
13. Rice GL, Bond J, Asipu A, et al. Mutations involved in Aicardi–Goutières syndrome implicate SAMHD1 as regulator of the innate immune response. *Nat Genet*. 2009;41:829-832.
14. Crow YJ, Black DN, Ali M, et al. Cree encephalitis is allelic with Aicardi-Goutières syndrome: implications for the pathogenesis of disorders of interferon alpha metabolism. *J Med Genet*. 2003;40: 183-187.
15. Sanchis A, Cerveró L, Bataller A, et al. Genetic syndromes mimic congenital infections. *J Pediatr*. 2005;146:701-705.
16. Burn J, Wickramasinghe HT, Harding B, Baraitser M. A syndrome with intracranial calcification and microcephaly in two sibs, resembling intrauterine infection. *Clin Genet*. 1986; 30:112-116.
17. Kalyanasundaram S, Dutta S, Narang A, Katariya S. Microcephaly with plate-like cortical calcification. *Brain Dev*. 2003;25: 130-132.
18. O'Driscoll MC, Daly SB, Urquhart JE, et al. Recessive mutations in the gene encoding the tight junction protein occludin cause band-like calcification with simplified gyration and polymicrogyria. *Am J Hum Genet*. 2010;87:354-364.
19. Weiss JL, Cleary-Goldman J, Tanji K, et al. Multicystic encephalomalacia after first-trimester intrauterine fetal death in monochorionic twins. *Am J Obstet Gynecl*. 2004;190: 563-565.

Epilepsia, 53(8):1441–1449, 2012
doi: 10.1111/j.1528-1167.2012.03548.x

FULL-LENGTH ORIGINAL RESEARCH

CASK aberrations in male patients with Ohtahara syndrome and cerebellar hypoplasia

***Hirotomo Saitsu, †Mitsuhiro Kato, ‡Hitoshi Osaka, §Nobuko Moriyama, ¶Hideki Horita, *Kiyomi Nishiyama, *Yuriko Yoneda, *Yukiko Kondo, *Yoshinori Tsurusaki, *Hiroshi Doi, *Noriko Miyake, †Kiyoshi Hayasaka, and *Naomichi Matsumoto**

*Department of Human Genetics, Yokohama City University Graduate School of Medicine, Kanazawa-ku, Yokohama, Japan; †Department of Pediatrics, Yamagata University Faculty of Medicine, Yamagata, Japan; ‡Division of Neurology, Clinical Research Institute, Kanagawa Children's Medical Center, Minami-ku, Yokohama, Japan; §Department of Pediatrics, Hitachi, Ltd., Hitachinaka General Hospital, Hitachinaka, Japan; and ¶Department of Pediatrics, Ibaraki Disabled Children's Hospital, Mito, Japan

Summary

Purpose: Ohtahara syndrome (OS) is one of the most severe and earliest forms of epilepsy. *STXBP1* and *ARX* mutations have been reported in patients with OS. In this study, we aimed to identify new genes involved in OS by copy number analysis and whole exome sequencing.

Methods: Copy number analysis and whole exome sequencing were performed in 34 and 12 patients with OS, respectively. Fluorescence in situ hybridization, quantitative polymerase chain reaction (PCR), and breakpoint-specific and reverse-transcriptase PCR analyses were performed to characterize a deletion. Immunoblotting using lymphoblastoid cells was done to examine expression of CASK protein.

Key Findings: Genomic microarray analysis revealed a 111-kb deletion involving exon 2 of *CASK* at Xp11.4 in a male patient. The deletion was inherited from his mother, who was somatic mosaic for the deletion. Sequencing of the mutant transcript expressed in lymphoblastoid cell lines derived from the patient confirmed the deletion of exon 2 in the mutant transcript with a premature stop codon. Whole exome sequencing identified another male patient who was harboring a c.1A>G mutation in *CASK*, which occurred de novo. Both patients showed severe cerebellar hypoplasia along with other congenital anomalies such as micrognathia, a high arched palate, and finger anomalies. No CASK protein was detected by immunoblotting in lymphoblastoid cells derived from two patients.

Significance: The detected mutations are highly likely to cause the loss of function of the CASK protein in male individuals. *CASK* mutations have been reported in patients with intellectual disability with microcephaly and pontocerebellar hypoplasia or congenital nystagmus, and those with FG syndrome. Our data expand the clinical spectrum of *CASK* mutations to include OS with cerebellar hypoplasia and congenital anomalies at the most severe end.

KEY WORDS: *CASK*, Ohtahara syndrome, Male, Cerebellar hypoplasia.

Ohtahara syndrome (OS), also known as early infantile epileptic encephalopathy with suppression-burst, is one of the most severe and earliest forms of epilepsy (Ohtahara et al., 1976). It is characterized by early onset of seizures, typically frequent epileptic spasms, seizure intractability, characteristic suppression-burst patterns on electroencephalography (EEG), and poor outcome with severe psychomotor retardation (Djukic et al., 2006; Ohtahara & Yamatogi, 2006). Brain malformations such as cerebral dysgenesis, hemimegalencephaly, Aicardi syndrome, and porencephaly are often associated with OS (Yamatogi & Ohtahara, 2002). However, mutations of the *ARX* and *STXBP1* gene have been reported in individuals with OS who showed no brain malformations, indicating that mutated genes are involved in OS (Kato et al., 2007, 2009; Fullston et al., 2010; Giordano et al., 2010; Saitsu et al., 2008, 2010).

CASK (Genbank accession number NM_003688.3) at Xp11.4 encodes a calcium/calmodulin-dependent serine protein kinase of 921 amino acids belonging to the membrane-associated guanylate kinase protein family (Hsueh, 2006). Accumulating evidence indicates that *CASK* is essential for synapse formation at both presynaptic and postsynaptic junctions. In addition, CASK enters the nucleus and regulates expression of genes involved in cortical development (Hsueh, 2006). Recently, heterozygous loss-of-function mutations in *CASK* were found in four female patients with X-linked intellectual disability (ID);

Accepted April 23, 2012; Early View publication June 18, 2012.
Address correspondence to Hirotomo Saitsu, Department of Human Genetics, Yokohama City University Graduate School of Medicine, 3-9 Fukuura, Kanazawa-ku, Yokohama 236-0004, Japan. E-mail: hsaitsu@yokohama-cu.ac.jp

microcephaly and pontocerebellar hypoplasia (MICPCH) and a hemizygous synonymous c.915G>A mutation, which caused skipping of exon 9 of *CASK* in about 20% of the mutant transcripts, was found in a male patient with the same disease and presentation (Najm et al., 2008). To date, 32 additional female cases have been reported, suggesting that ID, MICPCH, growth retardation, axial hypotonia with or without hypertonia of extremities, and optic nerve hypoplasia are caused by loss-of-function mutations of *CASK* in female cases (Moog et al., 2011; Hayashi et al., 2012). On the other hand, a missense mutation causing a partial skipping of exon 2 of *CASK* was found in affected male individuals in an Italian family with FG syndrome, which is characterized by multiple congenital anomalies and ID (Piluso et al., 2009). More recently, five missense mutations and a splice mutation, causing amino acid changes or in-frame deletions of the CASK protein, were found in male patients and variably affected carrier female patients with ID, often accompanied by congenital nystagmus (Tarpey et al., 2009; Hackett et al., 2010). Therefore it has been postulated that hypomorphic *CASK* alleles cause ID in male individuals. Collectively, mutations of *CASK* could cause a wide spectrum of ID, ranging from nonsyndromic mild ID to syndromic severe ID with structural brain abnormalities in both male and female patients.

Herein, we report on two male patients with OS, cerebellar hypoplasia, and multiple congenital anomalies. One patient had a *CASK* deletion and the other had a mutation at the translation initiation codon, both likely leading to a loss of CASK function. Detailed clinical and molecular data are presented.

Methods

Patients

A total of 34 Japanese patients (20 male and 14 female) with OS were analyzed for copy number aberrations. Twelve of them were additionally analyzed by whole exome sequencing. The diagnosis was made based on clinical features and characteristic patterns on EEG. Mutations in *STXBP1* were not identified in these patients (including Patients 1 and 2) by high-resolution melting analysis. Thirteen male patients, including Patient 1, and three female Patients were negative for *ARX* mutation. The experimental protocols were approved by the Yokohama City University School of Medicine Institutional Review Boards for Ethical Issues. Written informed consent was obtained from all individuals and/or their families in compliance with the relevant Japanese regulations.

Genomic microarray and cloning of deletion breakpoint

Genomic DNA obtained from peripheral blood leukocytes was used. Copy number alterations were studied by using Cytogenetics Whole-Genome 2.7M Array (Affymetrix, Santa Clara, CA, U.S.A.) for 30 patients and GeneChip Human Mapping 250K NspI (Affymetrix) for four patients. Copy number alterations were analyzed using the Chromosome Analysis Suite (ChAS; Affymetrix) with NA30.1 (hg18) annotations (for 2.7M Array) or using CNAG2.0 (for 250K) (Nannya et al., 2005). The junction fragment spanning the deletion was amplified by long polymerase chain reaction (PCR), using several primer sets based on putative breakpoints from the microarray data. The junction fragment was amplified using following primers: forward, 5′-ACCCAGCGTTTCACCAAGGTCTCT-3′; reverse, 5′-GTGGCTTCAGAATTAGGCCCACAAA-3′ (product size = 1,136 bp). PCR products were electrophoresed in agarose gels, stained with ethidium bromide, extracted from the gels using a QIAquick Gel extraction kit (Qiagen, Tokyo, Japan), and sequenced.

Quantitative real-time PCR

The deletion of *CASK* was analyzed using the patient's and parental genomic DNA by quantitative real-time PCR (qPCR) on a Rotor-Gene Q thermal cycling system (Qiagen). DNA extracted from two independent blood samples each from the patient and mother were used for analysis. PCR was performed in a volume of 15 μl containing 10 ng of genomic DNA, 1× Rotor-Gene SYBR Green PCR Master Mix (Qiagen), and 1.0 μM each primer. qPCR was carried out using the two standard curve relative quantification method with four standard samples including 30, 10, 3.33, and 1.11 ng DNA, respectively. Three primer sets for exons 2, 3, and 4 of *CASK*, and one reference primer set for an area on chromosome 9 were used. Relative copy number of test regions was calculated in comparison with that of the reference region. The experiments were independently repeated three times. The data were averaged, and the standard deviation was calculated. Primer information is available on request.

Fluorescent in situ hybridization (FISH)

RP11-977L20 covering the deletion of *CASK* was labeled with SpectrumGreen -11-dUTP (Abbott, Tokyo, Japan) by nick translation. Probe-hybridization mixtures (15 μl) were denatured at 70°C for 5 min, applied to chromosomes, incubated at 37°C for 20 h, and then washed and mounted with antifade solution (Vector Laboratories, Burlingame, CA, U.S.A.) containing 4,6-diamidino-2-phenylindole. Photographs were taken on an AxioCam MR Charge Coupled Device camera fitted to an Axioplan2 fluorescence microscope (Carl Zeiss, Tokyo, Japan). The mosaic ratio was examined by two independent investigators, who each counted 100 interphase nuclei.

RNA analysis

RNA analysis using lymphoblastoid cell lines was performed as described previously (Saitsu et al., 2011). Briefly, total RNA was extracted using an RNeasy Plus Mini Kit (Qiagen); 2 μg of total RNA was subjected to reverse transcription, and 1 μl of cDNA was used for PCR.

Primer sequences are ex1-F (5′-ATGTGTACGAGCTGT GCGAGGTGAT-3′) and ex4-R (5′-AGCGTCAGCTCGCT TTACGATTTCA-3′). Two separately extracted RNA samples were used in each duplicated experiment. The DNA in each PCR band was purified using a QIAquick Gel extraction kit (Qiagen) and sequenced.

Whole exome sequencing

DNAs were captured using the SureSelect^{XT} Human All Exon 50 Mb Kit (Agilent Technologies, Santa Clara, CA, U.S.A.) and sequenced with one lane per sample on an Illumina GAIIx platform (Illumina, San Diego, CA, U.S.A.) with 108-bp paired-end reads. Image analysis and base calling were performed by sequence control software real-time analysis and CASAVA software v1.7 (Illumina). A total of 94,106,348 paired-end reads were obtained for Patient 2 and aligned to the human reference genome sequence (GRCh37/hg19) using MAQ (Li et al., 2008) and NextGENe software v2.00 with sequence condensation by consolidation (SoftGenetics, State College, PA, U.S.A.). Single nucleotide variants (SNVs) were called using MAQ and NextGENe. Small insertions and deletions were detected using NextGENe. Called SNVs were annotated with SeattleSeq Annotation. The number of variants identified by exome sequencing in Patient 2 is shown in Table S1.

Immunoblotting

Lymphoblastoid cells were washed twice in ice-cold phosphate-buffered saline (PBS), and lysed in sodium dodecyl sulfate sample buffer. Samples were size-fractionated by sodium dodecyl sulfate–polyacrylamide gel electrophoresis, transferred to the polyvinylidene fluoride membrane, and analyzed with anti-CASK monoclonal antibody, which is produced by a synthetic peptide corresponding to residues surrounding Glu327 of human CASK protein (1:1,000 dilution, D24B12; Cell Signaling, Tokyo, Japan). Anti-Lamin B polyclonal antibody (1:500 dilution, sc-6217; Santa Cruz Biotechnology Inc., Santa Cruz, CA, U.S.A.) was used as a control. Secondary antibody was peroxidase-conjugated goat anti-rabbit IgG or bovine anti-goat IgG (Jackson ImmunoResearch, West Grove, PA, U.S.A.). Blots were detected using the Supersignal West dura (Pierce, Yokohama, Japan). Chemiluminescence was visualized using a FluorChem 8900 (Alpha Innotech, San Leandro, CA, U.S.A.). Experiments were repeated twice using two separately prepared samples.

Results

Clinical information

Patient 1 is a 4-year-old boy born to nonconsanguineous parents. The pregnancy was uneventful, and he was born at term (gestational age 41 weeks and 2 days) with induced labor but no asphyxia. His body weight was 2,606 g (−2.0 standard deviation [SD]), his height was 47.5 cm (−1.4 SD), and his head circumference was 32.2 cm (−1.2 SD). An apneic event with cyanosis, which was not improved by positioning or oxygen inhalation, was evident 2 days after birth. Brain magnetic resonance imaging (MRI) demonstrated prominent cerebellar hypoplasia (Fig. 1A). EEG showed multifocal epileptic discharges with a short period (1 s) of flat basic rhythm (Fig. 1C, left). Phenobarbital was administered at 21 days and was effective for the apneic event. At the age of 2 months, he developed daily clustering of tonic seizures with suppression-burst pattern on both awake and asleep EEG (Fig. 1C, right)and poor feeding. EEG at 5 months demonstrated hypsarrhythmia, which is characteristically seen in West syndrome. He exhibited long slender fingers, micropenis, micrognathia, and a short neck with obstructive respiration, and then required tracheostomy with laryngotracheal separation and gastrostomy. His head circumference was 47.1 cm (−2.7 SD) at 1 years and 4 months. On examination at 4 years, he was bedridden and unable to track objects. Tonic seizures lasting 10–30 s several times a day and frequent myoclonic seizures were seen regardless of treatment with phenobarbital, pyridoxal phosphate, zonisamide, clobazam, and lamotrigine. EEG during sleep at 3 years of age demonstrated multifocal sharp and slow-wave complexes and diffuse low-voltage fast-wave bursts or a desynchronization pattern.

Patient 2 is a 4-year-old boy born to nonconsanguineous parents. He was born at 39 weeks of gestation without asphyxia after uneventful pregnancy. His body weight was 2,000 g (−3.3 SD), his height was 43.0 cm (−2.8 SD), and his head circumference was 29.5 cm (−2.7 SD). He was poorly fed with milk and referred to us at 27 days after birth. Multiple anomalies were recognized such as micrognathia, high arched palate, shortened upper arms, bilateral overlapping fingers and clinodactyly, and persistent hypertrophic primary vitreous. He underwent ophthalmic surgery at 33 days after birth. Brain MRI demonstrated prominent cerebellar hypoplasia (Fig. 1B). At 3 months of age, he showed frequent generalized tonic seizures, and EEG showed a suppression-burst pattern in both awake and asleep states (Fig. 1D). He showed normal auditory brain responses. Laboratory data, including lactate, pyruvate, and very long fatty acids, were all normal. Phenobarbital was initiated and only partially effective for his seizures. Topiramate, clobazam, and sodium bromide were added, and seizure frequencies were decreased from daily to weekly. His development was severely delayed with no head control or eye pursuit. His deep tendon reflexes are exaggerated, with positive bilateral Babinski signs. He shows muscle hypertonus with rigidity of both upper and lower limbs.

Copy number analysis

Through screening for copy number alterations by genomic microarray analysis, we identified an approximately 110-kb microdeletion involving exon 2 of *CASK* at Xp11.4 in Patient 1 (Fig. 2A). Breakpoint-specific PCR analysis of

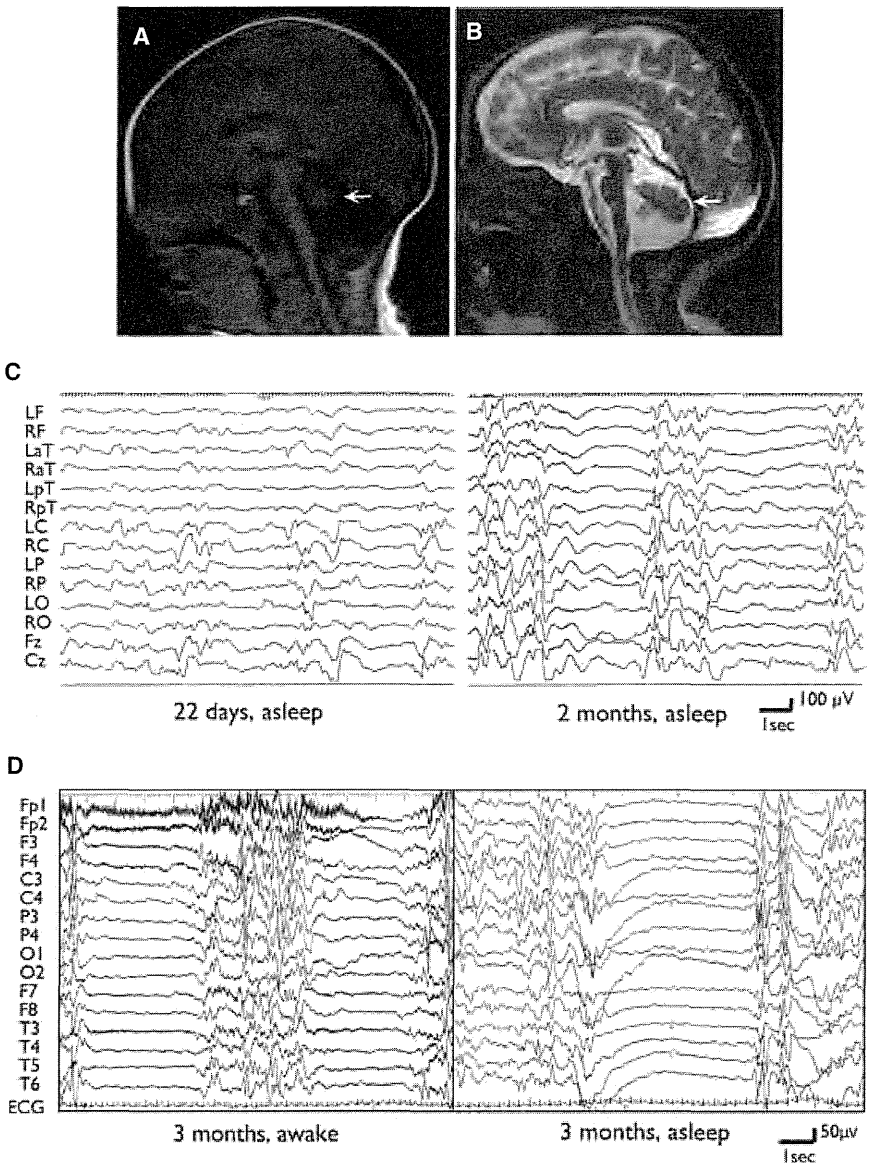

Figure 1.
Brain MRI findings in the patients. (**A**) T_1-weighted midline sagittal image of Patient 1 at age 21 days. (**B**) T_2-weighted midline sagittal image of Patient 2 at age 3 months. Both patients showed prominent cerebellar hypoplasia (arrows). (**C**) EEG of Patient 1 showed multifocal sharp wave or irregular sharp-and-slow wave complex but no diffuse epileptic discharges at age 22 days (left) and diffuse high-amplitude slow-wave burst mixed with irregular spike or sharp wave interrupted by low-amplitude activity (suppression-burst) at age 2 months (right). (**D**) EEG of Patient 2 at age 3 months. High-voltage bursts alternate with almost flat suppression phases at an approximately regular rate in both awake and asleep states.

the family showed that the deletion was inherited from his mother (Fig. 2B). The sequence of the junctional fragment confirmed a 111,172-bp deletion (NG_016754.1: g.17883_129055del) (Fig. 2C). Sequencing also identified 5-bp duplicated sequences as well as a 2-bp insertion at the deletion junction. We were surprised that the healthy mother possessed this deletion, because the deletion is predicted to lead to a frameshift with presumably premature termination of the translation. The deletion was further examined by qPCR and FISH analyses. Whereas the relative copy numbers of exons 3 and 4 (not deleted) were nearly 1.0 in the two maternal DNA samples, as expected, those for deleted exon 2 in the two samples were 0.67 and 0.81 (Fig. 2D). Because the relative copy number is expected to be 0.5 if one of two copies is deleted (as the healthy father showed), this result suggested that the mother may be somatic mosaic for the deletion. In fact, FISH analysis revealed that only 40 of 200 interphase nuclei showed one clear signal and another weaker signal, consistent with partial deletion within the bacterial artificial chromosome probe (Fig. 2E). Based on these findings, we concluded that the mother is somatic mosaic for the deletion, and that the percentage of mosaicism is approximately 20%. To explore the effect of the deletion on the transcription of *CASK*, reverse transcriptase PCR designed to amplify exons 1–4 was performed using total RNA extracted from lymphoblastoid cell lines (LCLs) derived from the patient and his mother (Fig. 2F). A single band (299-bp) corresponding to the wild-type *CASK* allele was amplified using a complementary DNA (cDNA) template from a control LCL (Fig. 2F). By contrast, only a smaller band, in which exon 2 had been deleted, was detected from the patient's cDNA

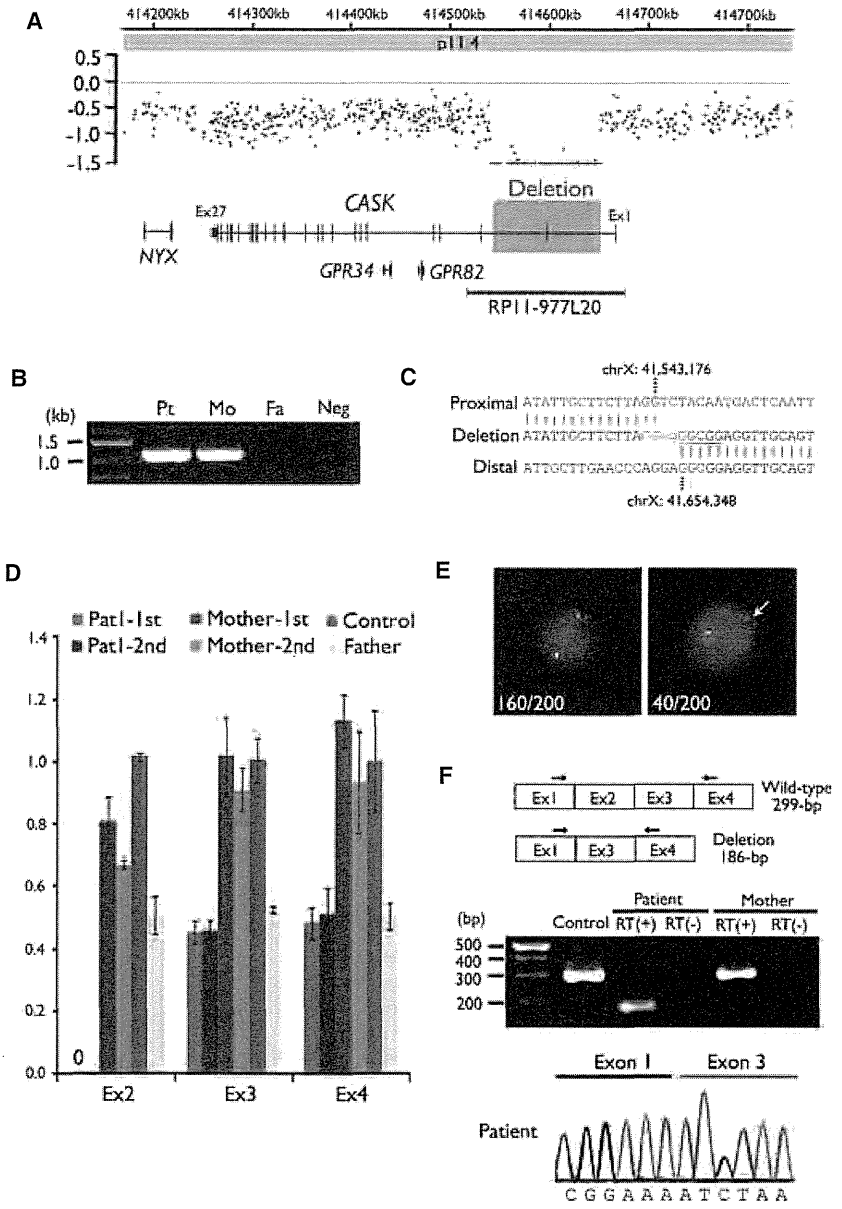

Figure 2.

A 111-kb deletion involving exon 2 of *CASK*. (**A**) The 2.7M array profile clearly shows a deletion involving exon 2 of *CASK* at Xp11.4. The x- and y-axes show the genomic location from the p telomere of chromosome X (UCSC coordinates, May, 2006) and $\log_2$ signal ratio values, respectively. Four RefSeq genes including *CASK* and RP11-977L20 clone used for FISH are shown. (**B**) Breakpoint-specific PCR analysis of the family. Primers flanking the deletion were able to amplify a 1,136-bp product from both the Patient 1 and his mother. Pt, patient; Mo, mother; Fa, Father; Neg, negative control (no template DNA). (**C**) Deletion junction sequence. Top, middle, and bottom strands show proximal, deleted and distal sequences, respectively. The two nucleotides inserted are presented in lower case. A 5-bp sequence that appears twice at the breakpoint region is colored red or underlined. (**D**) qPCR analysis of the family, and a female control. Two DNA samples extracted from two independent blood samples were used for analysis of the patient and his mother. Relative copy numbers of deleted exon 2 were 0.67 and 0.81 (both above 0.5) in the mother, suggesting somatic mosaicism of the deletion. (**E**) FISH images of RP11-977L20, covering the deletion, on the mother's chromosomes. One-hundred sixty nuclei showed two clear signals (left), and 40 nuclei showed one clear signal and a weaker signal (right, white arrow) consistent with partial deletion within the probe. (**F**) Schematic representation of the transcript from exons 1–4 of *CASK*. Exons and primers are depicted as boxes and arrows, respectively (top). A single wild-type amplicon was detected in a control and the mother. A smaller product was amplified only from the patient's cDNA. RT (+): with reverse transcriptase, RT (−): without reverse transcriptase as a negative control. Sequence of a smaller amplicon clearly demonstrated the exon 2 deletion (bottom).

(Fig. 2F). The smaller mutant band was not detected from the mother's cDNA (Fig. 2F). Human androgen receptor assay showed that X-inactivation was random (70:30) in the mother (data not shown). However, because the percentage of mosaicism was low (20%), it remains possible that the deletion allele may undergo X-inactivation in cells possessing it, leading to diminished expression of the deletion allele in LCL.

Whole exome sequencing

To find potential pathologic mutations, whole exome sequencing of 12 patients was performed. We focused on mutations in *CASK*, and identified a hemizygous c.1A>G mutation of the first ATG codon in Patient 2 (Fig. 3A,B). This mutation is anticipated to result in alternative ATG codon usage. By using the next downstream in-frame ATG codon positioned at c.202_204 (Fig. 3C), a truncated protein without the first 67 amino acids containing calmodulin-dependent kinase domain could be produced, although this ATG codon (CATATGC) does not conform to the Kozak consensus. The parental DNA did not have the mutation, suggesting that the mutation occurred de novo (Fig. 3B). No *CASK* mutations were found in any of the other patients.

Immunoblotting

To evaluate mutational effect for CASK expression in two patients, immunoblotting was performed using total lysate of LCL. A strong signal at 104 kDa was detected in a control and the mother of Patient 1, showing strong expression of wild-type CASK protein in LCLs (Fig. 4, top). However, both Patients 1 and 2 did not show any detectable signal (Fig. 4, top), whereas the Lamin B showed comparable expression in all samples loaded (Fig. 4, bottom). Thus these data suggest that expression of CASK protein was severely decreased in two patients.

Discussion

We describe two male patients possessing an intragenic *CASK* deletion (only exon 2) or a hemizygous c.1A>G

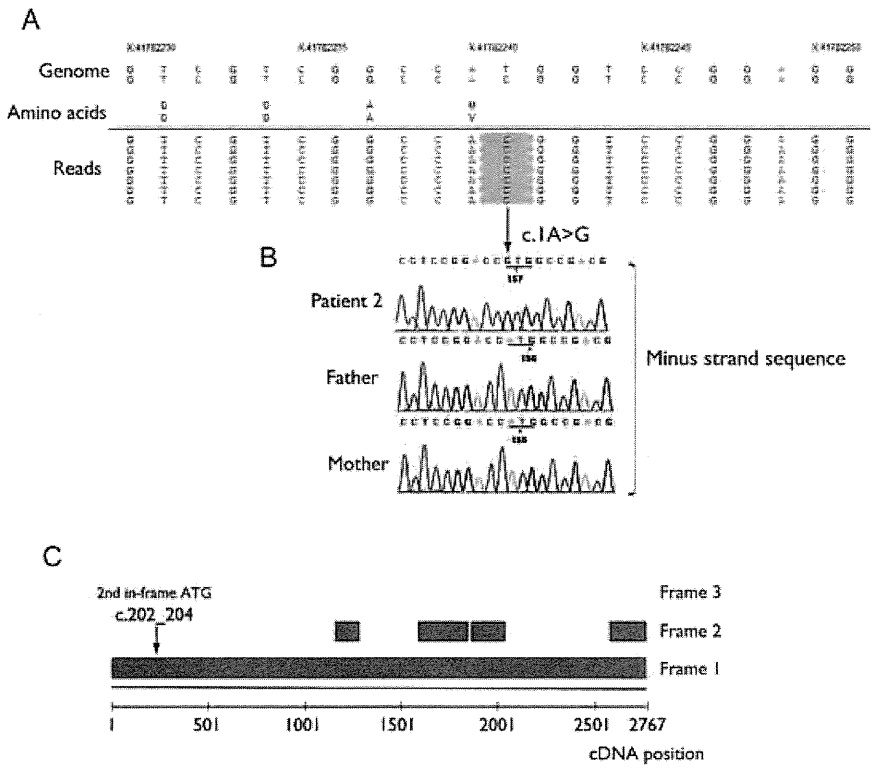

Figure 3.
c.1A>G mutation identified by exome sequencing. (**A**) From top to bottom, genomic sequence (plus strand), coding amino acids, and sequence reads covering the site of the pathogenic mutation. In genomic sequence and amino acids, upper and lower indicate reference and mutant alleles, respectively. There are six reads showing a hemizygous T>C transition at position 41,782,240 of chromosome X. (**B**) Validation of the c.1A>G mutation and inheritance analysis by Sanger sequencing. The mutation position is indicated by the arrow. (**C**) Possible open reading frames within the coding region of the *CASK* transcript (NM_003688.3). Open reading frames longer than 100 bp are shown in blue squares. The second in-frame ATG codon is positioned at c.202_204 (arrow). Any proteins longer than the protein utilizing the second in-frame ATG codon are not predicted.

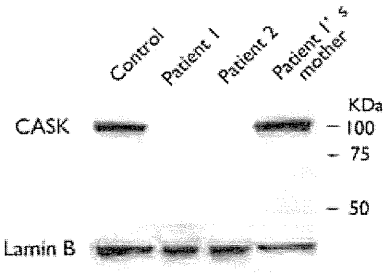

Figure 4.
Expression of CASK protein in LCL. Immunoblot analysis by using a monoclonal CASK antibody (top). Expression of CASK protein was not detected in LCL derived from two patients, whereas LCL of a control and Patient 1's mother showed strong CASK expression. The observed differences in expression were not due to difference of loading conditions, because the level of Lamin B protein was similar in all cases (bottom).

mutation. In Patient 1, the deletion is likely to be an almost null mutation as the mutant *CASK* transcript with exon 2 deletion has a frameshift with premature termination. Deletions in *CASK* have been reported in 16 female patients, and a skewed X-inactivation pattern was observed in two of them (the others had random inactivation pattern or not determined) (Froyen et al., 2007; Hayashi et al., 2008; Najm et al., 2008; Moog et al., 2011; Hayashi et al., 2012). Of interest, partial skipping of the exon 2 of *CASK* (approximately 3–6% of the unskipped transcripts) has been reported in male patients with FG syndrome showing ID, relative macrocephaly, hypotonia, severe constipation, and behavioral disturbance (Piluso et al., 2003, 2009). By contrast, our Patient 1 with complete deletion of exon 2 showed a more severe phenotype, suggesting that he showed one of the most severe phenotypes caused by *CASK* abnormalities. In Patient 2, the mutation of the first ATG codon could produce a truncated protein without the amino terminal 67 amino acids. However, this alternative in-frame ATG codon does not conform to the Kozak consensus, suggesting that its translation would be significantly reduced. In fact, CASK protein was not detected in the LCL of two patients, suggesting that expression of CASK protein should be extremely low. Because only partial skipping of exon 9 (about 20% of the mutant transcripts) (Najm et al., 2008) or of exon 2 (3–6% of the unskipped transcripts) (Piluso et al., 2009) is sufficient to cause ID and other features in male cases, it is likely that the maintenance of expression level of functional CASK protein is essential.

Two male patients with *CASK* abnormalities showed typical OS features, revealing an association between OS and *CASK* abnormalities in male patients, which has to date never been shown. Microcephaly and prominent cerebellar hypoplasia were also recognized, consistent with previous reports (Najm et al., 2008; Moog et al., 2011; Hayashi et al., 2012). Of interest, our patients also showed reduced body size and multiple congenital anomalies such as high arched palate, micrognathia, finger anomalies, and persistent hypertrophic primary vitreous. This suggests that *CASK* may be involved in overall body growth and development of these organs in humans. Supporting this idea, growth retardation and small jaw have been reported in patients with *CASK* abnormalities (Najm et al., 2008; Hackett et al., 2010; Moog et al., 2011). In addition, *CASK*-deficient mice showed micrognathia and cleft palate with male lethality (Laverty & Wilson, 1998), and hypomorphic *CASK* mutant mice are significantly smaller than littermate control mice (Atasoy et al., 2007). Therefore, it is likely that loss-of-function mutations in *CASK* cause reduced body size and multiple congenital anomalies, as well as OS and cerebellar hypoplasia.

The same deletion was found in both the mother and the affected son, indicating a germline mosaicism in the mother associated with recurrence risks. This information is useful for genetic counseling in the family. The maternal somatic mosaicism was confirmed by different methods including FISH, qPCR, and breakpoint-specific PCR analyses. We would like to emphasize the importance of breakpoint-specific PCR analysis, in which a specific band undoubtedly indicates the presence of the deletion allele. Because PCR is a powerful tool for amplifying target sequences, we could easily detect the somatic mosaic, even though it existed in approximately 20% of cells. In addition, it has been reported that PCR analyses of the deletion junction can detect extremely low-level mosaicism not detected by array comparative genomic hybridization (Zhang et al., 2009). The increasing density of available oligonucleotide arrays allows us to design long (or even regular) PCR primers for junctional cloning. Once junctional cloning is successful (though it is sometimes difficult), it is highly useful for examining parental states.

It has been determined that mutations in three genes (*STXBP1*, *ARX*, and *CASK*) cause OS. Screening for *STXBP1* mutations should be considered in OS patients with no brain anomalies in both male and female patients. Screening for *ARX* mutations would be reasonable in male patients with OS, and the presence of micropenis may encourage its screening (Kato et al., 2007). Based on this study, *CASK* mutations should be considered in patients with OS and cerebellar hypoplasia.

In conclusion, we report for the first time *CASK* abnormalities in male individuals with OS. Maternal somatic mosaicism of a *CASK* deletion is also described, suggesting that somatic and germline mosaicism of a microdeletion should be carefully considered in the examination of parental samples. Our data expand the clinical spectrum of *CASK* mutations to include OS with cerebellar hypoplasia and congenital anomalies at the most severe end of clinical presentation.

Epilepsia, 53(8):1441–1449, 2012
doi: 10.1111/j.1528-1167.2012.03548.x

Acknowledgments

We would like to thank the patients and their families for their participation in this study. This work was supported by Research Grants from the Ministry of Health, Labour and Welfare (H.S., M.K., H.O. N. Miyake, and N. Matsumoto), a Grant-in-Aid for Scientific Research from Japan Society for the Promotion of Science (M.K., H.O., N. Miyake, and N. Matsumoto), a Grant-in-Aid for Young Scientist from Japan Society for the Promotion of Science (H.S., H.D., and N. Miyake), a grant from the Japan Science and Technology Agency (N. Matsumoto), the Strategic Research Program for Brain Sciences (N. Matsumoto), and a Grant-in-Aid for Scientific Research on Innovative Areas (Foundation of Synapse and Neurocircuit Pathology) from the Ministry of Education, Culture, Sports, Science and Technology of Japan (N. Matsumoto), Research Grants from the Japan Epilepsy Research Foundation (H.S. and M.K.), a Research Grant from Naito Foundation (N. Matsumoto), and Research Grants from Takeda Science Foundation (N. Miyake and N. Matsumoto). This work was performed at the Advanced Medical Research Center, Yokohama City University, Japan.

Disclosure

None of the authors has any conflict of interest to disclose. We confirm that we have read the Journal's position on issues involved in ethical publication and affirm that this report is consistent with those guidelines.

References

Atasoy D, Schoch S, Ho A, Nadasy KA, Liu X, Zhang W, Mukherjee K, Nosyreva ED, Fernandez-Chacon R, Missler M, Kavalali ET, Sudhof TC. (2007) Deletion of CASK in mice is lethal and impairs synaptic function. *Proc Natl Acad Sci U S A* 104:2525–2530.

Djukic A, Lado FA, Shinnar S, Moshe SL. (2006) Are early myoclonic encephalopathy (EME) and the Ohtahara syndrome (EIEE) independent of each other? *Epilepsy Res* 70(Suppl. 1):S68–S76.

Froyen G, Van Esch H, Bauters M, Hollanders K, Frints SG, Vermeesch JR, Devriendt K, Fryns JP, Marynen P. (2007) Detection of genomic copy number changes in patients with idiopathic mental retardation by high-resolution X-array-CGH: important role for increased gene dosage of XLMR genes. *Hum Mutat* 28:1034–1042.

Fullston T, Brueton L, Willis T, Philip S, MacPherson L, Finnis M, Gecz J, Morton J. (2010) Ohtahara syndrome in a family with an ARX protein truncation mutation (c.81C>G/p.Y27X). *Eur J Hum Genet* 18:157–162.

Giordano L, Sartori S, Russo S, Accorsi P, Galli J, Tiberti A, Bettella E, Marchi M, Vignoli A, Darra F, Murgia A, Bernardina BD. (2010) Familial Ohtahara syndrome due to a novel *ARX* gene mutation. *Am J Med Genet A* 152A:3133–3137.

Hackett A, Tarpey PS, Licata A, Cox J, Whibley A, Boyle J, Rogers C, Grigg J, Partington M, Stevenson RE, Tolmie J, Yates JR, Turner G, Wilson M, Futreal AP, Corbett M, Shaw M, Gecz J, Raymond FL, Stratton MR, Schwartz CE, Abidi FE. (2010) *CASK* mutations are frequent in males and cause X-linked nystagmus and variable XLMR phenotypes. *Eur J Hum Genet* 18:544–552.

Hayashi S, Mizuno S, Migita O, Okuyama T, Makita Y, Hata A, Imoto I, Inazawa J. (2008) The *CASK* gene harbored in a deletion detected by array-CGH as a potential candidate for a gene causative of X-linked dominant mental retardation. *Am J Med Genet A* 146A:2145–2151.

Hayashi S, Okamoto N, Chinen Y, Takanashi JI, Makita Y, Hata A, Imoto I, Inazawa J. (2012) Novel intragenic duplications and mutations of CASK in patients with mental retardation and microcephaly with pontine and cerebellar hypoplasia (MICPCH). *Hum Genet* 131:99–110.

Hsueh YP. (2006) The role of the MAGUK protein CASK in neural development and synaptic function. *Curr Med Chem* 13:1915–1927.

Kato M, Saitoh S, Kamei A, Shiraishi H, Ueda Y, Akasaka M, Tohyama J, Akasaka N, Hayasaka K. (2007) A longer polyalanine expansion mutation in the *ARX* gene causes early infantile epileptic encephalopathy with suppression-burst pattern (Ohtahara Syndrome). *Am J Hum Genet* 81:361–366.

Kato M, Koyama N, Ohta M, Miura K, Hayasaka K. (2009) Frameshift mutations of the *ARX* gene in familial Ohtahara syndrome. *Epilepsia* 51:1679–1684.

Laverty HG, Wilson JB. (1998) Murine CASK is disrupted in a sex-linked cleft palate mouse mutant. *Genomics* 53:29–41.

Li H, Ruan J, Durbin R. (2008) Mapping short DNA sequencing reads and calling variants using mapping quality scores. *Genome Res* 18:1851–1858.

Moog U, Kutsche K, Kortum F, Chilian B, Bierhals T, Apeshiotis N, Balg S, Chassaing N, Coubes C, Das S, Engels H, Van Esch H, Grasshoff U, Heise M, Isidor B, Jarvis J, Koehler U, Martin T, Oehl-Jaschkowitz B, Ortibus E, Pilz DT, Prabhakar P, Rappold G, Rau I, Rettenberger G, Schluter G, Scott RH, Shoukier M, Wohlleber E, Zirn B, Dobyns WB, Uyanik G. (2011) Phenotypic spectrum associated with CASK loss-of-function mutations. *J Med Genet* 48:741–751.

Najm J, Horn D, Wimplinger I, Golden JA, Chizhikov VV, Sudi J, Christian SL, Ullmann R, Kuechler A, Haas CA, Flubacher A, Charnas LR, Uyanik G, Frank U, Klopocki E, Dobyns WB, Kutsche K. (2008) Mutations of CASK cause an X-linked brain malformation phenotype with microcephaly and hypoplasia of the brainstem and cerebellum. *Nat Genet* 40:1065–1067.

Nannya Y, Sanada M, Nakazaki K, Hosoya N, Wang L, Hangaishi A, Kurokawa M, Chiba S, Bailey DK, Kennedy GC, Ogawa S. (2005) A robust algorithm for copy number detection using high-density oligonucleotide single nucleotide polymorphism genotyping arrays. *Cancer Res* 65:6071–6079.

Ohtahara S, Yamatogi Y. (2006) Ohtahara syndrome: with special reference to its developmental aspects for differentiating from early myoclonic encephalopathy. *Epilepsy Res* 70(Suppl. 1):S58–S67.

Ohtahara S, Ishida T, Oka E, Yamatogi Y, Inoue H, Karita S, Ohtsuka Y. (1976) [On the specific age dependent epileptic syndrome: the early-infantile epileptic encephalopathy with suppression-burst.]. *No to Hattatsu* 8:270–279.

Piluso G, Carella M, D'Avanzo M, Santinelli R, Carrano EM, D'Avanzo A, D'Adamo AP, Gasparini P, Nigro V. (2003) Genetic heterogeneity of FG syndrome: a fourth locus (FGS4) maps to Xp11.4-p11.3 in an Italian family. *Hum Genet* 112:124–130.

Piluso G, D'Amico F, Saccone V, Bismuto E, Rotundo IL, Di Domenico M, Aurino S, Schwartz CE, Neri G, Nigro V. (2009) A missense mutation in *CASK* causes FG syndrome in an Italian family. *Am J Hum Genet* 84:162–177.

Saitsu H, Kato M, Mizuguchi T, Hamada K, Osaka H, Tohyama J, Uruno K, Kumada S, Nishiyama K, Nishimura A, Okada I, Yoshimura Y, Hirai S, Kumada T, Hayasaka K, Fukuda A, Ogata K, Matsumoto N. (2008) De novo mutations in the gene encoding STXBP1 (MUNC18-1) cause early infantile epileptic encephalopathy. *Nat Genet* 40:782–788.

Saitsu H, Kato M, Okada I, Orii KE, Higuchi T, Hoshino H, Kubota M, Arai H, Tagawa T, Kimura S, Sudo A, Miyama S, Takami Y, Watanabe T, Nishimura A, Nishiyama K, Miyake N, Wada T, Osaka H, Kondo N, Hayasaka K, Matsumoto N. (2010) *STXBP1* mutations in early infantile epileptic encephalopathy with suppression-burst pattern. *Epilepsia* 51:2397–2405.

Saitsu H, Hoshino H, Kato M, Nishiyama K, Okada I, Yoneda Y, Tsurusaki Y, Doi H, Miyake N, Kubota M, Hayasaka K, Matsumoto N. (2011) Paternal mosaicism of an *STXBP1* mutation in OS. *Clin Genet* 80:484–488.

Tarpey PS, Smith R, Pleasance E, Whibley A, Edkins S, Hardy C, O'Meara S, Latimer C, Dicks E, Menzies A, Stephens P, Blow M, Greenman C, Xue Y, Tyler-Smith C, Thompson D, Gray K, Andrews J, Barthorpe S, Buck G, Cole J, Dunmore R, Jones D, Maddison M, Mironenko T, Turner R, Turrell K, Varian J, West S, Widaa S, Wray P, Teague J, Butler A, Jenkinson A, Jia M, Richardson D, Shepherd R, Wooster R, Tejada MI, Martinez F, Carvill G, Goliath R, de Brouwer APM, van Bokhoven H, Van Esch H, Chelly J, Raynaud M, Ropers H-H, Abidi FE, Srivastava AK, Cox J, Luo Y, Mallya U, Moon J, Parnau J, Mohammed S, Tolmie JL, Shoubridge C, Corbett M, Gardner A, Haan E, Rujirabanjerd S, Shaw M, Vandeleur L, Fullston T, Easton DF, Boyle J, Partington M, Hackett A, Field M, Skinner C, Stevenson RE,

Bobrow M, Turner G, Schwartz CE, Gecz J, Raymond FL, Futreal PA, Stratton MR. (2009) A systematic, large-scale resequencing screen of X-chromosome coding exons in mental retardation. *Nat Genet* 41:535–543.

Yamatogi Y, Ohtahara S. (2002) Early-infantile epileptic encephalopathy with suppression-bursts, Ohtahara syndrome; its overview referring to our 16 cases. *Brain Dev* 24:13–23.

Zhang F, Khajavi M, Connolly AM, Towne CF, Batish SD, Lupski JR. (2009) The DNA replication FoSTeS/MMBIR mechanism can generate genomic, genic and exonic complex rearrangements in humans. *Nat Genet* 41:849–853.

Supporting Information

Additional Supporting Information may be found in the online version of this article:

Table S1. All variants identified by exome sequencing in Patient 2.

Please note: Wiley-Blackwell is not responsible for the content or functionality of any supporting information supplied by the authors. Any queries (other than missing material) should be directed to the corresponding author for the article.

Epilepsia, 53(8):1441–1449, 2012
doi: 10.1111/j.1528-1167.2012.03548.x

RESEARCH ARTICLE

AMERICAN JOURNAL OF medical genetics PART A

Ophthalmic Features of CHARGE Syndrome With CHD7 Mutations

Sachiko Nishina,[1] Rika Kosaki,[2] Tatsuhiko Yagihashi,[3] Noriyuki Azuma,[1] Nobuhiko Okamoto,[4] Yoshikazu Hatsukawa,[5] Kenji Kurosawa,[6] Takahiro Yamane,[7] Seiji Mizuno,[8] Kinichi Tsuzuki,[9] and Kenjiro Kosaki[3,10]*

[1]Division of Ophthalmology, National Center for Child Health and Development, Tokyo, Japan

[2]Division of Medical Genetics, National Center for Child Health and Development, Tokyo, Japan

[3]Department of Pediatrics, Keio University School of Medicine, Tokyo, Japan

[4]Department of Medical Genetics, Osaka Medical Center and Research Institute for Maternal and Child Health, Osaka, Japan

[5]Department of Ophthalmology, Osaka Medical Center and Research Institute for Maternal and Child Health, Osaka, Japan

[6]Division of Medical Genetics, Kanagawa Children's Medical Center, Kanagawa, Japan

[7]Division of Ophthalmology, Kanagawa Children's Medical Center, Kanagawa, Japan

[8]Department of Genetics, Institute for Developmental Research, Aichi Human Service Center, Aichi, Japan

[9]Department of Ophthalmology, Aichi Children's Health and Medical Center, Aichi, Japan

[10]Center for Medical Genetrics, Keio University School of Medicine, Tokyo, Japan

Received 26 December 2010; Accepted 25 October 2011

Coloboma and various ocular abnormalities have been described in CHARGE syndrome, although the severity of visual impairment varies from case to case. We conducted a multicenter study to clarify the ophthalmic features of patients with molecularly confirmed CHARGE syndrome. Thirty-eight eyes in 19 patients with CHARGE syndrome and confirmed CHD7 mutations treated at four centers were retrospectively studied. Colobomata affected the posterior segment of 35 eyes in 18 patients. Both retinochoroidal and optic disk colobomata were bilaterally observed in 15 patients and unilaterally observed in 3 patients. The coloboma involved the macula totally or partially in 21 eyes of 13 patients. We confirmed that bilateral large retinochoroidal colobomata represents a typical ophthalmic feature of CHARGE syndrome in patients with confirmed CHD7 mutations; however, even eyes with large colobomata can form maculas. The anatomical severity of the eye defect was graded according to the presence of colobomata, macula defect, and microphthalmos. A comparison of the severity in one eye with that in the other eye revealed a low-to-moderate degree of agreement between the two eyes, reflecting the general facial asymmetry of patients with CHARGE syndrome. The location of protein truncation and the anatomical severity of the eyes were significantly correlated. We suggested that the early diagnosis of retinal morphology and function may be beneficial to patients, since such attention may determine whether treatment for amblyopia, such as optical correction and patching, will be effective in facilitating the visual potential or whether care for poor vision will be needed.

Key words: CHARGE syndrome; *CHD7*; coloboma; ophthalmic features

How to Cite this Article:
Nishina S, Kosaki R, Yagihashi T, Azuma N, Okamoto N, Hatsukawa Y, Kurosawa K, Yamane T, Mizuno S, Tsuzuki K, Kosaki K. 2012. Ophthalmic features of CHARGE syndrome with CHD7 mutations.
Am J Med Genet Part A 158A:514–518.

INTRODUCTION

CHARGE syndrome is a multiple malformation syndrome named from the acronym of its major features: coloboma, heart defects, atresia of the choanae, retarded growth and/or development, genital anomalies, and ear abnormalities [Pagon et al., 1981; Zentner et al., 2010]. The major ocular feature of CHARGE syndrome is coloboma, and a previous investigation by ophthalmologists revealed an incidence of up to 86%, although the severity

Grant sponsor: Ministry of Health, Labour and Welfare, Tokyo, Japan.
*Correspondence to:
Kenjiro Kosaki, M.D., Ph.D., Department of Pediatrics, Keio University School of Medicine, 35 Shinanomachi, Shinjuku-ku, Tokyo 160-8582, Japan. E-mail: kkosaki@z3.keio.ac.jp
Published online 2 February 2012 in Wiley Online Library (wileyonlinelibrary.com).
DOI 10.1002/ajmg.a.34400

of coloboma and visual impairment varied from case to case [Russell-Eggitt et al., 1990].

Recently, the gene *Chromodomain helicase DNA-binding protein-7* (*CHD7*) at chromosome 8q12.1 was identified as a causative gene of CHARGE syndrome [Vissers et al., 2004]. Up to 70% of patients clinically diagnosed as having CHARGE syndrome exhibit mutations in the *CHD7* gene [Aramaki et al., 2006a; Jongmans et al., 2006; Lalani et al., 2006]. Although the exact function of this gene product remains unknown, it may have an important effect on an early stage of ocular morphogenesis.

We conducted the present multicenter study to clarify the ophthalmic features of patients with molecularly confirmed CHARGE syndrome and to explore the role of *CHD7* in ocular development.

PATIENTS AND METHODS

Thirty-eight eyes in 19 patients clinically diagnosed as having CHARGE syndrome at the National Center for Child Health and Development, the Osaka Medical Center and Research Institute for Maternal and Child Health, the Kanagawa Children's Medical Center, or the Institute for Developmental Research, Aichi Human Service Center were retrospectively studied. All the patients had been molecularly confirmed to carry *CHD7* mutations at the Keio University School of Medicine [Aramaki et al., 2006a]. The clinical diagnosis of CHARGE syndrome was made based on the Blake criteria [Blake et al., 1998]. Molecular screening for mutations in the *CHD7* gene was conducted as reported previously [Aramaki et al., 2006b]. Ophthalmic features were examined using slit-lamp biomicroscopy and binocular indirect ophthalmoscopy. Two patients were also examined using a spectral domain optical coherence tomography (SD-OCT). The SD-OCT images were obtained with RS-3000 (NIDEK Co., Ltd., Gamagori, Japan). The best-corrected visual acuity (BCVA) was measured with a standard Japanese VA chart using Landolt rings or pictures at 5 m, then converted to Snellen VA.

The anatomical severity of the eye defect was classified as follows: Grade 1, Normal; Grade 2, colobomata with macular formation; Grade 3, colobomata including the macula; and Grade 4, colobomata, macular defect, and microphthalmos. Then, Cohen's kappa coefficient [Cohen, 1960] was used to measure the agreement of the severity in the two eyes among 19 CHD7-mutation positive patients. The potential correlation between the anatomical severity of the eyes in an individual and the amino acid position where the truncation of the *CHD7* protein occurred in the same individual was evaluated among 14 patients with protein-truncating mutations.

This study was approved by the institutional ethics committee; the patients or the parents of the patients provided informed consent prior to enrollment in the study.

RESULTS

The characteristics of the 38 eyes of the 19 patients with CHARGE syndrome carrying *CHD7* mutations are summarized in Table I. Ten patients (53%) were male and 9 (47%) were female. The age of the patients at the time of the examination ranged from 1 to 21 years (mean 7.9 ± 5.0 years). Ocular abnormalities were found in 18 patients (94.7%), bilateral abnormalities were observed in 17 patients (89.4%), and unilateral abnormalities were observed in 1 patient (5.3%). Among these 18 patients, all 35 abnormal eyes had varying severities of colobomata.

TABLE I. Characteristics of Patients of CHARGE Syndrome With CHD7 Mutations (n = 9)

Variable	Number
Gender	
Male	10 (53%)
Female	9 (47%)
Age at examination	1–21 years
Mean	7.9 ± 5.0 years
Ocular abnormalities (colobomata)	
Bilateral	17 (89.4%)
Unilateral	1 (5.3%)
None	1 (5.3%)
BCVA	
<20/400	4 (21.1%)
20/400 to <20/60	7 (36.8%)
20/60 to 20/20	6 (31.6%)
Not measured	2 (10.5%)

BCVA, best-corrected visual acuity.

The ocular features of the individual patients are summarized in Table II. Colobomata affected the posterior segment in 35/38 eyes (92.1%), retinochoroidal coloboma was present in 33 eyes (86.8%), and optic disk coloboma was present in 33 eyes (86.8%). Both retinochoroidal coloboma and optic disk coloboma were bilaterally present in 15 patients (78.9%) and unilaterally present in 3 patients (15.8%). The coloboma involved the macula totally or partially in 21 eyes (55.3%) of the 13 patients (68.4%): bilaterally in 8 patients

TABLE II. Ocular Features of the Patients (n = 19 patients, 38 eyes)

	Number of patients (%)			Number of
Findings	Bilateral	Unilateral	Total	eyes (%)
Colobomata	17 (89.5)	1 (5.3)	18 (94.7)	35 (92.1)
Retinochoroidal	15 (78.9)	3 (15.8)	18 (94.7)	33 (86.8)
Optic disk	15 (78.9)	3 (15.8)	18 (94.7)	33 (86.8)
Macula	8 (42.1)	5 (26.3)	13 (68.4)	21 (55.3)
Iris	1 (5.3)	0 (0.0)	1 (5.3)	2 (5.3)
Lens	0 (0.0)	1 (5.3)	1 (5.3)	1 (2.6)
Microphthalmos	3 (15.8)	2 (10.5)	5 (26.3)	8 (21.1)
Microcornea	3 (15.8)	1 (5.3)	4 (21.1)	7 (18.4)
Ptosis	1 (5.3)	1 (5.3)	2 (10.5)	3 (7.9)
PFV	0 (0.0)	1 (5.3)	1 (5.3)	1 (2.6)
Cataract	0 (0.0)	1 (5.3)	1 (5.3)	1 (2.6)
High myopia (>6.0 D)	2 (10.5)	1 (5.3)	3 (15.8)	5 (13.2)

PFV, persistent fetal vasculature.